ALMA MATER STUDIORUM-UNIVERSITÀ DI BOLOGNA

_____

CAMPUS DI CESENA

SCUOLA DI INGEGNERIA E ARCHITETTURA

Corso di Laurea Magistrale in Ingegneria Biomedica

TESI DI LAUREA

in

MECCANICA DEI TESSUTI BIOLOGICI

QUANTITATIVE ASSESSMENT OF BONE QUALITY AFTER TOTAL HIP REPLACEMENT THROUGH MEDICAL IMAGES:

2D AND 3D APPROACHES

CANDIDATO

Jonathan Pitocchi

RELATORE

Chiar.mo. Prof. *Luca Cristofolini*

CORRELATORI

Prof. *Paolo Gargiulo*
Prof. *Magnús Kjartan Gíslason*

Anno Accademico 2015/16

III° Sessione

A mio nipote,

Nicholas

Abstract

Bone quality evaluation is an important step in the clinical field, both in pathological and non-pathological conditions. In particular, in patients undergoing Total Hip Replacement, the presence of the prosthesis alters the physiological stress conditions of the femur, causing a process of bone adaptation that can have consequences on implant stability and bone conditions. Therefore, it is evident the importance of monitoring the quality of the bone surrounding the stem, both in short and long term period.

Starting from densitometric measurements on CT images, this thesis tackles two main topics: 1) improvement of current protocol to evaluate bone mineral density changes (three-dimensionally around the prosthesis) 1 year after the operation and application to a large dataset (11 patients) to examine the differences between subjects; 2) feasibility study on 8 patients of novel 2D approaches based on standard cross-sectional slices of femur, in order to obtain a tool for bone quality evaluation which can be affordable for the clinicians, but also minimally invasive for the patients, by reducing the radiation dose.

The results of the 3D approach suggest that it may be used as a monitoring tool during the follow-up. Moreover the thesis shows the feasibility of the new 2D approaches, although some limits need to be overcome to use them in a clinical ambit.

Keywords: Total Hip Replacement; Bone Remodeling; Bone Mineral Density; 2D and 3D assessment; Bone profile.

Abstract

La valutazione della qualità dell'osso è un passo importante nel campo clinico, sia in condizioni patologiche che non patologiche. In particolare, in pazienti sottoposti ad intervento di sostituzione totale d'anca, la presenza della protesi altera le condizioni di stress fisiologiche del femore, causando un processo di adattamento dell'osso che può avere conseguenze sulla stabilità dell'impianto e sulle condizioni dell'osso. Perciò, è evidente l'importanza di monitorare la qualità dell'osso che circonda lo stelo, sia nel breve che nel lungo termine.

A partire da rilevazioni densitometriche effettuate su immagini TC, questa tesi affronta due argomenti principali: 1) miglioramento del protocollo corrente per la valutazione della variazione di densità minerale ossea (tridimensionalmente attorno alla protesi) dopo un anno dall'operazione e applicazione ad un ampio dataset (11 pazienti) per esaminare le differenze tra soggetti; 2) studio di fattibilità su 8 pazienti di nuovi approcci 2D basati su sezioni standard del femore, con lo scopo di ottenere uno strumento per la valutazione della qualità dell'osso che possa essere affidabile per i clinici, ma anche minimamente invasivo per i pazienti, riducendo la dose di radiazione.

I risultati dell'approccio 3D suggeriscono che può essere usato come strumento di monitoraggio post-operatorio del paziente. Inoltre la tesi mostra la fattibilità di nuovi approcci 2D, sebbene alcuni limiti devono essere superati prima di poterli utilizzare in ambito clinico.

Parole Chiave: Sostituzione Totale d'Anca; Rimodellamento Osseo; Densità Minerale Ossea; Valutazione con approcci 2D e 3D; Profilo Osseo.

Contents

Overview

Bone quality evaluation is an important step in the clinical field, both in pathological and non-pathological conditions. Having a better knowledge on how the bone is adapting to different situations, can strongly improve the diagnostic phase, helping clinicians in the decision making.

Nowadays, there are different cases in which medical images are used to assess the quality of bone structures, e. g., DEXA has become the standard technique to quantify Bone Mineral Density, providing an accurate method to diagnose osteoporosis. More recently, many studies have shown how qCT (quantitative Computed Tomography) can be the starting point in the analysis of damaged or diseased tissues [1] [2] [3] [4].

In this interesting field, most current research is focusing on improving the aspects of instrumentation design, image processing software, data acquisition procedures and computational modeling, to obtain a tool which can be affordable for the clinicians, but also minimally invasive for the patients, by reducing radiation dose.

With regards to the main subject of this work, similar remarks may be made about the evaluation of bone quality in subjects undergoing Total Hip Replacement (THR). This orthopedic surgical procedure is one of the most used and most successful in the world, restoring the functionality of the hip-joint articulation and increasing life expectancies [5]. THR consists of replacing the acetabulum and the femoral head with two different components. There are two methods to perform the operation: in the first case, *bone cement* is used to fix the prosthesis (CEMENTED), instead in the second one, a *press-fitting* procedure allows the primary stability between implant and bone (UNCEMENTED). Although this operation offers immediate free movement and pain-relief, many clinical problems are highlighted in the literature. The presence of the prosthesis in fact alters the physiological stress conditions of the femur, causing a process of bone adaptation that can have consequences on implant stability.

Many factors are involved in the mechanism of bone remodeling: these includes not only patient-related factors (such as gender, patient activity, general health), but also prosthesis-related factors (type of fixation, geometry of the implant, position). Based on these considerations, it is evident the importance of monitoring the quality of the bone surrounding the stem, both in short and long term period. [6]

This thesis is part of a large project [7] involving Landspítali – University Hospital of Iceland and Reykjavík University, that aims to introduce novel approach, acquire unique data and suggest patient specific evaluation to optimize implant technology and clinical assessment. As a result of this collaboration, a protocol to evaluate bone mineral density changes around the prosthesis one year after surgery has been already created and qualitatively validated. [8]

Through this process, unlike every other technique carried out to study bone density changes (like DEXA), it is possible to have volumetric measures of bone growth/loss and to see how these changes are distributed in the bone's model. Anyway, such a method requires access to the full-bone CT-scans acquisition, both for Post24 and Post1y dataset, thus limiting its applicability in the clinical field. For these reasons, the possibility to extract the same information from single, standardized slices, is a main goal to pursue, both for clinical advantages and ethical issues.

This thesis tackles two main topics: 1) improvement of the previous protocol for 3D gain/loss evaluation and application to a large dataset to examine the main differences between subjects 2) feasibility study of novel 2D approaches based on standard cross-sectional slices of femur.

For the 2D approach, 5 CT-scans are selected (both for dataset Post24 and Post1y) and then examined in two different ways:

a) *Gain/Loss assessment using Matlab Image Processing Toolbox:* using the image process toolbox of Matlab, it is possible to overlay the images and replicate the 3D approach, showing, just in the slice, how Bone Mineral Density (BMD) changes 1 year after the operation. This method is potentially easier to apply in the clinical field, especially in the region of the femur where bone gain and loss are greater.

b) *2D Bone Profile:* through a model fitting of the Density Distribution of the 5 CT-scans (HU-n° of pixels), it is possible to extract some parameters that can be used for bone quality assessment.

1. Introduction

The main purpose of this chapter is to introduce the basic information about the anatomy and the biomechanical properties of bones and the nature of THR surgery. Moreover, the fundamental principles of Computed Tomography are described in order to better understand the procedures analyzed in the thesis, along with its purpose in bone quality assessment.

1.1 The Bone

1.1.1 Bone Physiology

Bone is a specialized form of connective tissue in which the extracellular matrix is mineralized, thus conferring stiffness and mechanical strength to the skeleton while still leaving some degree of elasticity. Although it is a living tissue, it is composed (on a weight basis) by 2/3 of inorganic component (such as *calcium carbonates* and *phosphates*) and by 1/3 of organic component (principally *collagen*, but also *lipids*, *proteoglycans* and *cells)*. The organic part is the tough and flexible component while the mineral is the brittle and stiff one.

The bone has two important and distinct functions:

-physiological function: it acts as a mineral reservoir for calcium homeostasis, in order to keep constant its level in the blood under different physical and metabolic activity; moreover, it provides an environment for marrow (both blood forming and fat storage),

-mechanical function: it protects the vital organs and, in synergy with muscles, consents the motion of the entire body.

Bone has a strongly hierarchical organization. (Fig 1.1)

Focusing on a nanostuctural scale, it is possible to distinguish the presence, within the collagen fibrils, of little crystals of *hydroxyapatite (HA)*, namely *calcium apatite*, $Ca_{10}(PO_4)_6(OH)_2$, (length: 20-40 nm; thickness: 1.5-5 nm) pointed on the same direction of the collagen fibers, thus influencing the mechanical properties of the bone. At a microscopic level, parallel collagen fibers are organized into layers called *lamellae* (thickness: 3–7 μm). Lamellae put near each other have different orientations, building a ply-wood like structure.

In the cortical bone, a group of 4-20 concentric lamellae are arranged to surround a central cavity, the *Haversian canal* (which contains vessels and bone nerves), forming a cylindrical system called *osteon* (with a diameter of 150-250 μm). [9]
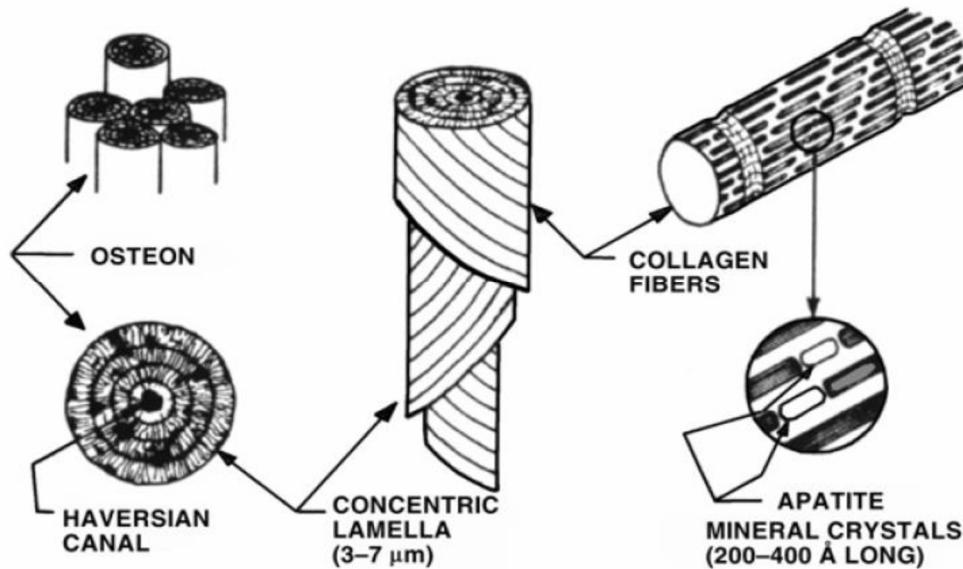

Fig. 1.1: Hierarchical levels of the cortical bone [10]

The highest hierarchical level includes two main bone types: *cortical* (or *compact*) and *trabecular* (*spongy* or *cancellous*). (Fig 1.2) One of the difference is linked to the contents of marrow and soft tissue: less than the 10% of the volume in cortical bone, almost the 75% of volume in cancellous bone.
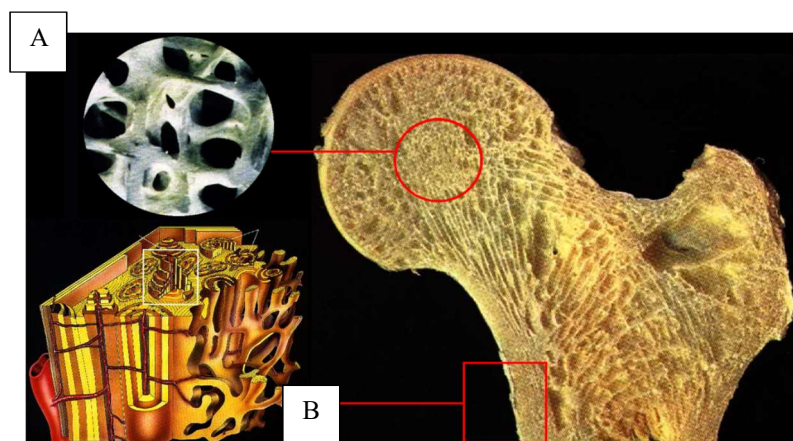
Fig. 1.2: Trabecular (A) and Cortical (B) Bone in proximal femur

Image 1.2 shows also a substantial diversity between the two organizations, thus influencing the mechanical properties. Cortical bone is dense and consists of aligned osteons while trabecular bone is highly porous with spongy appearance in which lamellae are arranged in small struts called *trabeculae* (thickness < 0.2 mm). Cortical bone is heavier, stiffer and stronger, while trabecular one is lighter, less dense and with low mechanical strength properties.

4

1.1.2 Bone Remodeling

Bone remodeling is the complex of concurring biological process that lead to bone geometry and bone density changes. The first analysis of this mechanism is attributed to Julius Wolff who proposed a mathematical formulation (Wolff's law) to describe how the bone adapts and forms its architecture according to the externally loads applied, in order to maintain a physiological stress-strain state. (Fig. 1.3)
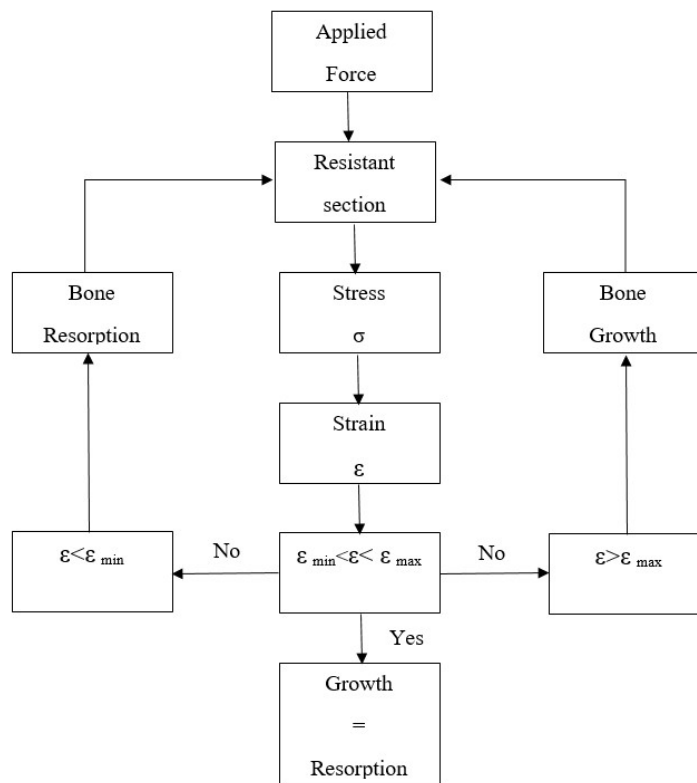

Fig. 1.3 Possible phenomenology of bone remodeling. Adapted from [11]

Figure 1.3 shows a possible phenomenology of bone remodeling, as a result of a mechanical stimulus. Considering that σ is the stress in the resistant section following an applied force and ε the associated strain, if the strain is above or below a threshold defined by the physiological levels, bone starts a process of adaptation which leads to a prevalence of *growth* or *resorption*. In particular, if ε is under a minimum value, cortical bone's thickness decreases in order to have a smaller resistant section and trabeculae's number and dimension are reduced, along with a demineralization of the matrix (*resorption*). On the other hand, if ε exceeds a maximum value, bone remodels in the opposite way (*growth*).

This process is always present and is fundamental not only for removal and repair damaged bone, but also to maintain integrity of the adult skeleton and mineral homeostasis. [12]

The mediators of bone remodeling are the cells that populate bone tissue. O*steoblasts* (mono-nuclear) can be stimulated to increase bone mass. They are able to synthetize and release a non-mineralized matrix, called *osteoid*. O*steoclasts* are the only cells capable of resorbing bone. They are typically multinucleated and can attack HA through an acidification of the environment. *Osteocytes* can be defined as the sensors of the process. They are former osteoblast trapped in the just produced osteoid and lead the action of osteoblasts and osteoclast. The remodeling is obtained with a continuous process in which osteoclasts reabsorb old bone and osteoblasts create new matrix. Main steps are shown in figure 1.4.
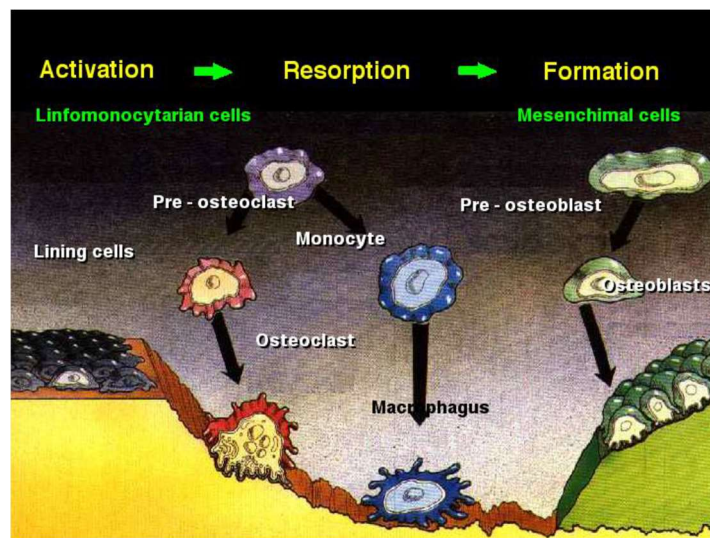

Fig. 1.4: Activation, Resorption, Formation in bone remodeling

First osteoclasts are activated, thus starting the resorption phase that lasts approximately 10 days. Following resorption, macrophage cells are present in the remodeling site. Pre-osteoblast are then recruited. After the differentiation in mature osteoblasts, they begin to secrete new osteoid matrix that then mineralizes to form new bone. The complex balance between bone resorption and formation is guided by interrelated factors such as genetic, mechanical, vascular, nutritional, hormonal, and local. [13]

Bone remodeling allows the human skeleton to adapt to different load situations. In particular, looking to the arrangement of cortical and trabecular bone in the proximal femur, it is possible to see how, especially the trabeculae, are optimized to resist to the daily forces conditions. Moreover, the epiphysis can absorb a great amount of energy in case of an impact due to a sideway fall. (Fig. 1.5) The alignment of osteons and trabeculae respond also to a metabolic necessity: in fact at this

arrangement correspond at the same time a minimum amount of material and a minimum risk of damage.
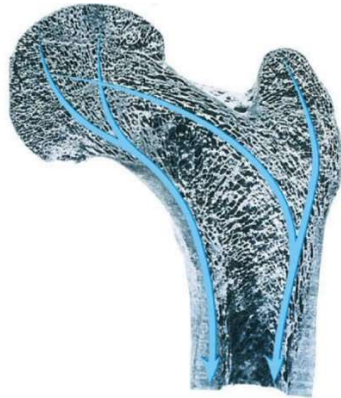

Fig. 1.5 Direction of stresses created by body weight, muscles forces and joint force

Copyright McGraw-Hill Companies, Inc

Focusing on the effects of a total hip replacement on this optimization, it is clear that the presence of the stem (which is much stiffer than the surrounding bone), modifies the loading conditions with respect to the preoperative situation. The principal consequence is an alteration, induced by the metal implant, of the normal stress patterns that lead the bone remodeling. This phenomenon is called *stress shielding*. Figure 1.6 shows how load is transferred from the pelvis to the femur after THR. The stress-shielding leads to an imbalance of the bone remodeling, causing bone resorption around the stem, because the metal shields the bone from the stresses, potentially compromising implant stability [15]. At the tip of the stem instead there is not a demineralization and, on the contrary, bone growth is encouraged (the prosthesis transfers the load it is subject).
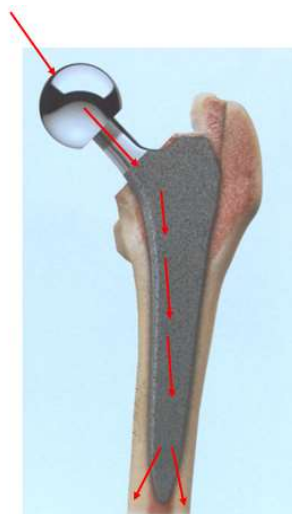

Fig. 1.6 Image showing how load is transferred from the pelvis to the femur after THR. The stem is stiffer than the bone, this causes stress shielding in the proximal femur, with consequent bone mineral density decrease. Femur remains dense distally to the stem.

1.1.3 Anatomy of the femur

The femur belongs to the category of long bones and it is the longest between the 206 bones in the adult skeleton.

As shown in fig. 1.7, it typically consists of a central part, tube-shaped, called *diaphysis*, in which a shell of cortical bone surrounds the trabecular one.
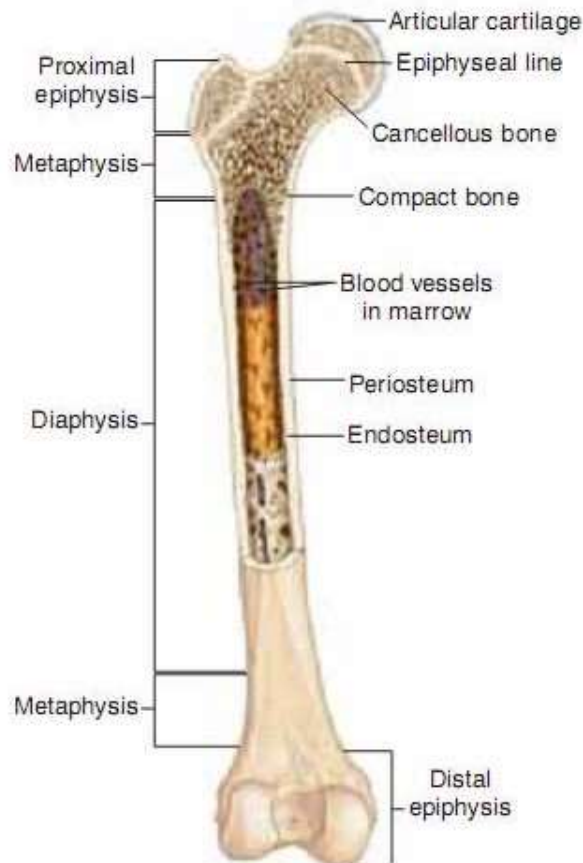
Fig. 1.7: Anatomy of the femur

Approaching the joints, an intermediate region, the *metaphysis*, connects the diaphysis to the *epiphysis*, covered by articular cartilage (hyaline) that allows the relative movement of adjacent bone segment, reducing the friction between the surfaces.

The outer layer of the cortical bone is called *periosteum*. It contains active cells that enlarge the diameter of bones in remodeling.

The canal in the middle of long bones is called the *medullary canal*. The surfaces of these canals are called *endosteum*, which mainly consists of laminated cells. [10] Also in the endosteum the remodeling is strong hence having a pivotal role in bone-formation.

1.1.4 The Hip Joint

The hip joint (coxal) is one of the most important and most flexible joint in the human skeleton. It is a synovial ball-and-socket which connects the lower limb to the pelvic girdle.

The ball is the head of the femur (hemispherical) which fits into the acetabulum (a cup-shaped socket in the pelvis). As a joint cavity, the touching surfaces are covered with articular cartilage, providing a smooth surface for the movement of the bones; moreover, it has a synovial membrane producing synovial fluid. (Fig. 1.8)

The presence of strong muscles and ligaments that connect the ball to the socket leads to a great stability of the joint. In this way, it can transfer the loads to the legs both in static (e.g. standing) and dynamic (e.g. walking) postures. Especially during running and jumping, the force of the body's movements multiplies the force on the hip joint to many times the force exerted by the body's weight. The hip joint has to be able to resist to these extreme forces repeatedly during intense physical activities.

Biomechanically, the hip joint has a very high range of motion. The ball-and-socket structure allows flexion/extension, abduction/adduction and medial/lateral rotation.
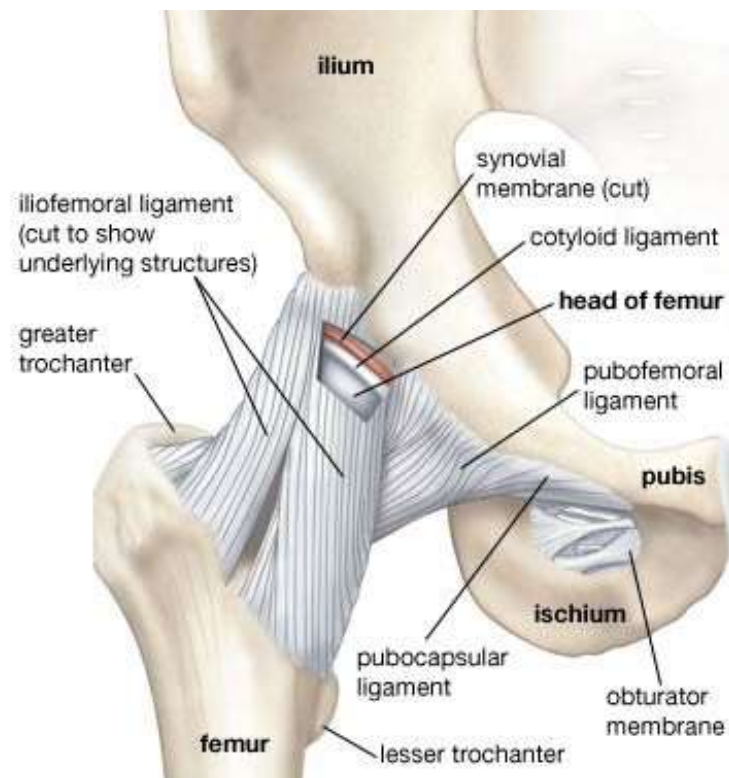

Fig. 1.8 Anatomy of the hip joint, showing attachment of the principal ligaments [16]

1.2. Total Hip Replacement (THR)

1.2.1 Introduction

Total Hip Replacement is one of the of the most common surgery done on the human musculoskeletal system today and with increasing life expectancies in many populations worldwide, also the number of operation will continue to raise. [5] Its success is also due to the fact that it offers immediate free movement and pain-relief, restoring the functionality of the hip joint.

There are different reasons which cause subjects to undergo a THR. For example, in a study from 2001 that involved 101 patients, frequent complaints were: walking (68%), pain (58%), limping (36%), night pain and walking stairs (both 35%) [17].

Looking in the literature for the medical condition that usually lead to THR, one of the most common diagnosis is osteoarthrosis (OA). [18] [19] OA is a wear-related type of joint disease, generally found in elderly people. It consists of a mechanical breakdown of the cartilage which is linked to sever pain during daily living activities. OA affects the entire joint, but the part that principally suffers is the articular cartilage that allows the femoral head to moving into the acetabulum without friction.

Other diseases requiring THR include: *Rheumatoid arthritis (AR)*, where the cartilage is damaged because of chronic inflammation; *Avascular necrosis*, where blood supply to the femoral head is limited, causing the bone to collapse; *Paget's Disease*, a metabolic bone disorder that induces an increased and irregular formation of bone; *Developmental Dysplasia*, in which femoral head has an abnormal relationship to the acetabulum; *Tumor*; *Femur's neck Fracture*. [20]

The popularity of this surgical operation is confirmed by study on the population undergoing THR. (Fig 1.9)

The statistics from Emilia Romagna (Italy) [19] and the rest of the OECD countries [21] show that the number of hip replacements has augmented rapidly since 2000. On average, the rate of hip replacements increased by about 35% between 2000 and 2013.
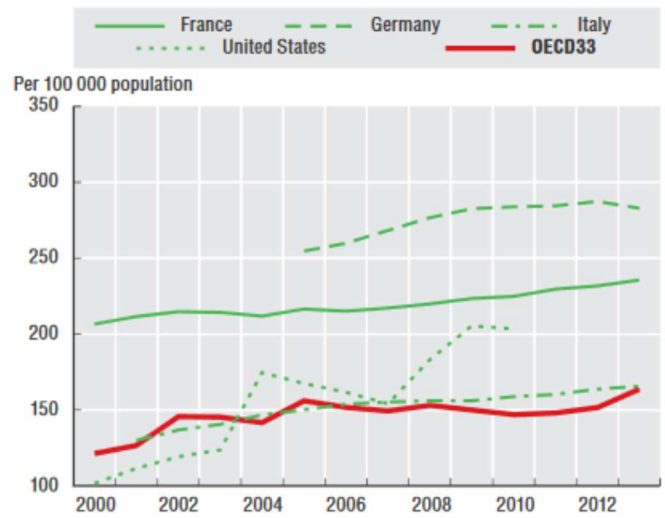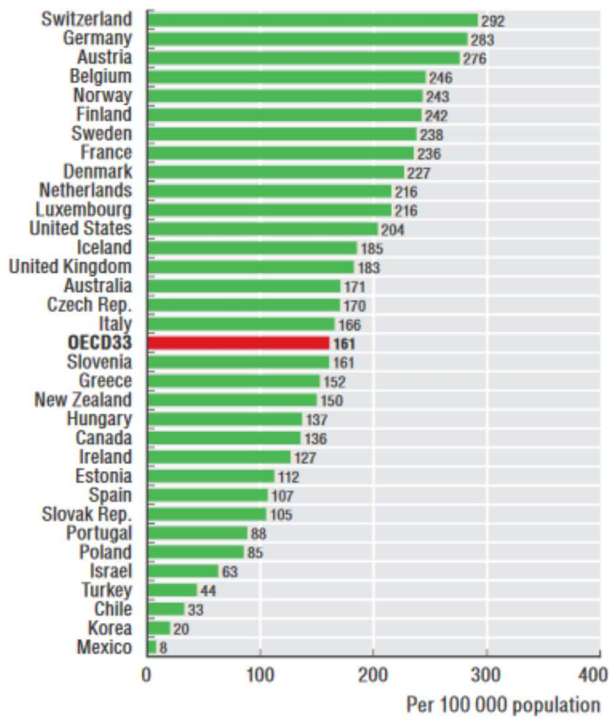
Fig. 1.9. Left: Number of THR surgeries in 2013. Iceland counts 185 operations per 100 000 people, Italy 166;

Right: Trend in hip replacement surgery, for some selected countries, from 2000 to 2013. Average statistics for OECD countries are represented in red.

Analyzing the data collected between 2000 and 2014 in Emilia Romagna, the average age for the first THR was 66.7 years.

The majority of the subjects who received the implant is female (60% of the patients undergoing THR during the period 2000-2014). The statistics highlight also that the average age for male was 66.5 while for female was 70.2.

1.2.2 Prosthesis Components and Surgery

Prosthesis for THR have been the object of a continuous research in order to limit the complications after the surgery, this way leading to a large variety of stems on the market, classified according to shape, material, coating etc. Today however, it is possible to define a basic modular-design common for all the implants. (Fig. 1.10)

The prosthesis is generally composed by two modules: the hip one (*shell + liner*), anchored to bone of the pelvis and the leg one (*femoral head + femoral stem*), which is inserted in the femur.

The liner is put into the shell to allow a smooth movement between the surfaces. This component represents the socket of the artificial joint. The femoral head instead is the ball and it rotates within the liner.
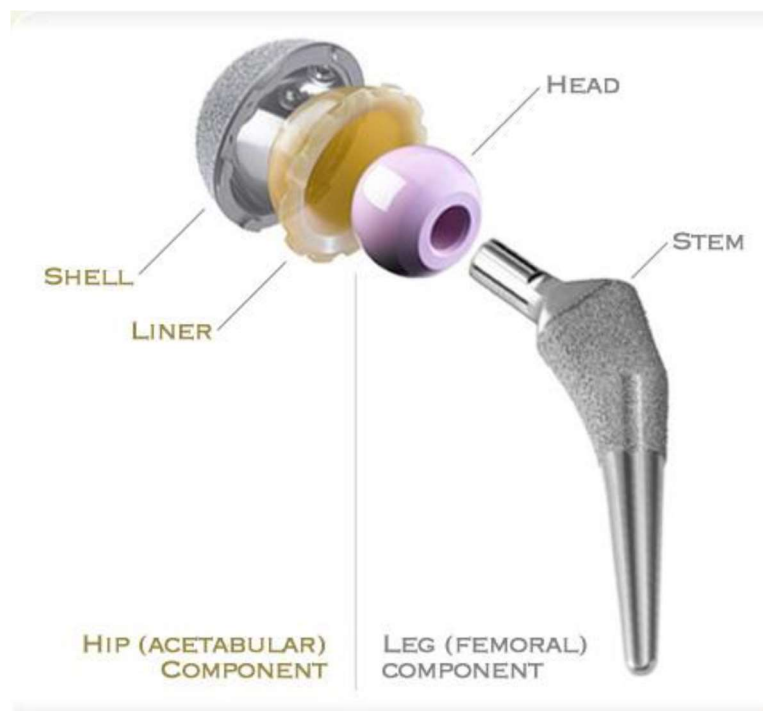
Fig. 1.10. Components of THR. [22]

Currently, there are two methods used to fix the implant: with cement (*cemented*) and through press-fit (*uncemented*).
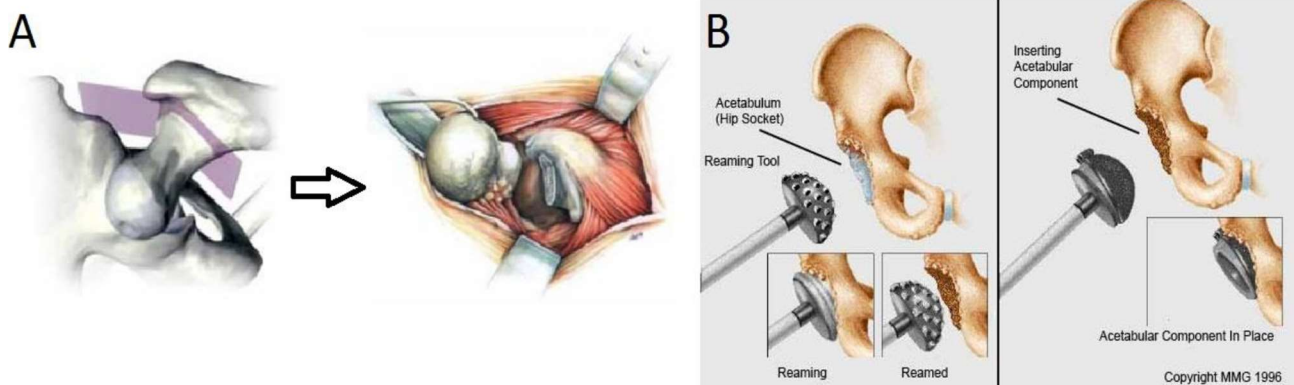

Fig. 1.11 (A) Femoral neck removal [23] (B) Articular cartilage in the acetabulum removed with reamer [24]

The surgical operation follows standard steps. Firstly, the femoral head and part of the neck is removed (osteotomy, Fig. 1.11, a). Regarding the hip preparation, a rasp/reamer is used to clean the articular cartilage thus leading to securely fix the acetabular component. (Fig. 1.11, b)

At this point, femur needs to be prepared to receive the stem. The procedure differentiates for cemented and uncemented approach.

For cemented implant, the stem is fixed through an acrylic bone cement. In general, the material for the cement is Polymethylmethacrylate (PMMA). The surgeon, using a reamer, creates a cavity into the femur, he removes the spongy bone in the medullary canal, then he compresses and removes the bone with a rasp. At the beginning, smaller rasp sizes are used until templated size of the stem is reached. The final size of the rasp is bigger than the stem to leave space for cement. [23] Moreover, a bone plug (called cement restrictor) is inserted into the canal to prevent the cement from flowing along the distal part of the femur.

Bone cement is injected into the prepared femoral canal. In this phase, it is extremely important that the cement is distributed in a homogenous way, in order to avoid implant loosening and to decrease the risk of periprosthetic fractures. Having stem with smooth surface helps the success of the surgery, cause local peaks of stress may lead to cracks in cement layers. (Fig. 1.12)
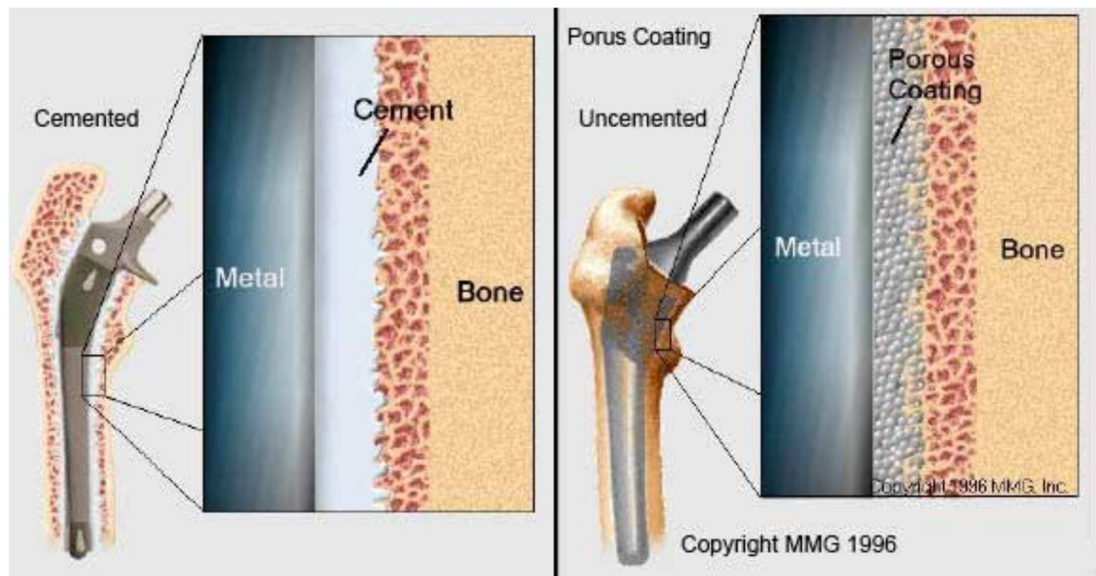
Figure 1.12: Cemented implant (left). Uncemented implant (right) [25]

For uncemented implant, the press-fit contact between implant and surrounding bone is employed to anchor the stem (*Primary stability)*. Additionally, the induced bone ingrowth into the porous surface of the prosthesis leads to a more solid fixation (*Secondary stability*). (Fig. 1.12)

The surgeons, through hammering blows, fixes and inserts the stem. He needs to be really carefully in terms of force, since an excessive load may result in a fracture.

1.2.3 Comparison between Cemented and Uncemented Implant Fixation

After a brief description of THR surgical procedure and of the two typologies of implant fixation, it is necessary to examine how the femur is affected by the presence of the prosthesis. In this way, it is possible to highlight the importance of the bone quality assessment not only in the pre-operative decision making, but also in the follow-up of the patient.

In fact, despite the success of both cemented and uncemented implant, today there is not an absolute criterion for choosing between these methodological options. Utilizing the cemented approach provides a better primary stability, thanks to the presence of a cement layer between the implant and the bone. Moreover, the presence of the cement reduces the stress-shielding.

Anyway, the bone resorption generated by stress-shielding increases the periprosthetic fracture risk and can lead to stem's aseptic loosening, which is reported as one of the major reason for implant failure. [26] [27]

14

On the other hand, without the use of cement, prosthetic primary stability is achieved thanks to the geometrical inter-locking, the press-fit and the friction between femur and stem, while secondary stability is secured by the bone adaptation of the layers adjacent to the prosthesis. In fact they are preloaded and this stress encourage a process of bone growth into the surface texture of femoral component (*osteointegration*). [28]

Although the continuous research in this field, because of the great number of implants, many subjects undergoing THR need revision 10 or 15 years after the operation. In the first years post-operatively instead, non-cemented implants are more frequently revised, due to the periprosthetic fracture. Anyway, the revision surgery for press-fit procedure is easier, with fewer complications than revision surgeries for cemented implants. [29] [30] In fact, when the prosthesis and the cement are removed, a part of the inside of the femur follows, thus having bad consequences on bone strength.

Considering the revision rate for infection instead, similar outcomes are shown for both the uncemented and the cemented fixation with antibiotic cement. [31]

As described in § 1.2.2, a critical phase during press-fit is when the surgeon hammers the stem into the bone. It is important that the clinicians check bone quality because with a low bone mineral density or an important disease (like osteoporosis) the bone may not be able resist to the forces produced with the hammering, thus leading to an intra-operative fracture. For this reason, uncemented implant is usually chosen for younger and more active patients, while for older and less active patient the cemented option is more safe. Anyway, other factors have an impact the decision making, such as gender, bone mineral density, stem design, gait patterns.

1.3 Basic principles of Computed Tomography

Computed Tomography (CT) has become through the years a very powerful tool in medical imaging, using X-rays to provide an image that is based on the linear absorption coefficients of the tissues through which they pass. In this way, it is possible to obtain a series of cross-sectional slices of the body in which distinguish different structures depending on their density. Every CT image is the result of two different steps: first scan data acquisition and then tomographic reconstruction trough computational processing. [32] [33] [34]

The image is acquired by a rapidly rotating x-ray tube around the patient. The radiation that is not absorbed by the body is measured by detectors and the final image is generated by reconstruction from the multiple x-ray projections through complex algorithms. (Fig. 1.13)
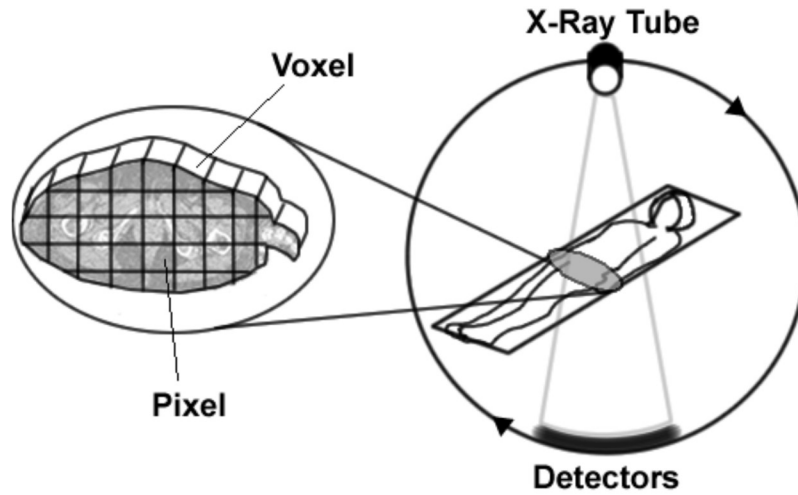

Fig. 1.13: Simplified schematic image of CT data acquisition

All CT images are formed by voxels, which are volume elements. Every voxel is described by a CT value. It is the average value of all linear attenuation coefficients and reflects how much the energy of the x-ray beam is reduced when going through the tissue, contained within that particular voxel. Since the attenuation coefficients can vary between CT scan models and different settings on the same scanner, the Hounsfield Unit scale (HU) is used to standardize them. The HU is defined based on the attenuation coefficient of each voxel, compared to attenuation coefficient of the water and of air as described by formula 1.1.

$$HU = 1000 \times \frac{\mu_X - \mu_{Water}}{\mu_{Water} - \mu_{Air}} \qquad [1.1]$$

μ_X is the average attenuation coefficient of the voxel, μ_{Water} is the attenuation coefficient of water and μ_{Air} is the attenuation coefficient of air. The Hounsfield Unit scale is based on a normalized index where air is defined to have value of -1000 HU and water the value of zero HU. Since attenuation depends on the density of the scanned volume it is possible to distinguish between hard and soft tissue is possible.

Moreover, calibrating the CT scanner with a phantom allows to define the relationship between HU and BMD, as it will be examined in § 2.1.3.

One voxel can contain different types of tissues due to the finite spatial resolution of the imaging tool. This phenomenon generates the so-called partial volume effect (PVE). Regarding this work, PVE is one of the main problem during the segmentation process. In fact, at the interface between a softer and a harder tissue (i.e. cortical bone and muscles) the edge may appear as blurred and it is more difficult to separate the tissues.

1.4 Bone quality evaluation

As already explained, bone quality plays a pivotal role in the success of THR. Clinical assessment of bone material distribution is an important factor in determining the treatment for patients or to monitor the changes in bone quality over a period of time. It is inevitable that the bone will undergo changes in morphology and strength following a THR procedure. It is however important to be able to monitor where the changes occur to determine if the bone density decreases (loss) or if it increases (gain).

Along with mechanical test [35] [36], different approaches based on medical images are becoming very useful, giving the possibility to extract information to improve planning and post-operative assessment.

Measuring bone mineral density in vivo for example, can provide quantitative information on bone's quality, that can be used for several applications. Along with plain radiographic absorptiometry and dual energy X-ray absorptiometry (DEXA), quantitative computed tomography (CT) represents a good tool to measure BMD. In fact, quantitative CT is the most reproducible and accurate method for in vivo assessment of cortical and cancellous bone density. [37] [38] Moreover, is the only technique that provides a three-dimensional volumetric analysis, since it provides a series of cross-sectional images.

Starting from CT-scans, it is possible, through a standard segmentation based on opportune threshold of the CT-HU, to separate bone from other tissue and apply noninvasive approach to measure BMD. This procedure can be used in different way, giving the possibility to monitor density changes both in healthy and operated leg of the same patient and differentiate the results by implant technique and gender versus subject's age. [39]

Similar analysis it's critical in the pre-operative evaluation, in order to optimize prosthesis selection. As already described, clinicians have not guidelines when choosing between cemented or uncemented procedure, so usually they rely on experience or simple patient metrics such as age and sex. Different studies show that such information alone is not enough for providing optimal decision on the implant technology to employ, highlighting the importance of a correct evaluation of BMD. [40] [41] [42] [43]

1.5 Aim of the thesis

An approach based on CT-scans offers different modality to evaluate bone quality, not only in the THR field. However, in comparison to another standard method, such DEXA, subjects undergo higher radiation dose (0.5-1.0 mSv against 0.001-0.1 mSv). [44] This may represent a limit in the clinical application, cause, especially today, there is an increasing need to obtain tools that are affordable but also minimally invasive for patients.

For this reason, the principal aim of the thesis is to investigate novel 2D approaches, using standard CT-scans acquired 24 hours and 1 year after total hip arthroplasty, in order to create an ethically compatible method that can be used in the clinical field to examine bone quality

After performing an improvement of the 3D evaluation for BMD changes developed at Reykjavik University, the protocol is, for the first time, applied to a set of cemented patients. This way, a comparison between the volumetric bone growth/loss in subjects with different type of implant fixation is possible, increasing the number of application of the method.

Moreover, through a selection of 5 slices in the regions of interest of the femur, a new technique based on the analysis of the Density Distribution of the CT-scan (HU values-N° of pixels) is applied to 8 uncemented subjects. The results have been compared to the 3D approach, showing the outcomes of such approach and determining advantages and disadvantages of each method.

The slices of the same 8 patients have been also processed with an alternative procedure which allows to visualize and quantify the bone gain/loss in single images through a more automated image registration provided in Matlab.

This thesis wants to test the feasibility of a bone quality assessment based on few slices, moving the first steps to make this kind of investigation more sustainable both for clinicians and patients.

2. Materials and Methods

This section contains all the steps needed to reproduce the analysis with other subjects in the future. The chapter is divided in four parts. In the first one are presented the information about subjects involved and protocol of acquisition (CT-scan, CT-calibration, Metal artefact reduction). Then, three different protocol for the assessment of bone quality are described, along with the tools used in the evaluation.

2.1 Data

2.1.1 Subjects Information

Currently, a total of 75 patients are enrolled in the project of the RU named "*Clinical evaluation score for Total Hip Arthroplasty planning and post-operative assessment*". The criteria for being included were that patients could not have had a previous THA or total knee arthroplasty (TKA). Anyway, for this study, 11 subjects have been selected from the entire cohort, 7 females and 4 males. 8 received an uncemented implant, 3 a cemented one. The youngest patient was 48 years old and the oldest 65. The implant selection for the patients was in the hands of their operating surgeon who based their selection on patient's age, gender and general physical conditions.

The average age is 56.3 ± 6.6 years. For males, the average age is 51.8 ± 5.6, while for females the average age is 58.9 ± 6.0 years. All the information about patients' gender, age and type of implant are summarized in the Table 2.1.

Patient n°	Age	Sex	Type of implant
1	60	F	Uncemented
2	48	F	Uncemented
3	50	M	Uncemented
4	61	F	Uncemented
5	48	M	Uncemented
6	49	M	Uncemented
7	54	F	Uncemented
8	60	M	Uncemented
9	60	F	Cemented
10	64	F	Cemented
11	65	F	Cemented

Table 2.1: Patient's info

2.1.2 CT Acquisition

All the subjects were scanned with a *Philips Brilliance 64 Spiral-CT* (Fig. 2.1) three times: 1-3 days before, 24 hours and 1 year after the surgery. However, for the purpose of this project, only 24h and post1y dataset was utilized.

The scan protocol included slice thickness of 1 mm, slice increment of 0.5 mm and a tube intensity of 120 KVp.

Fig. 2.1: Philips Brilliance 64-slice CT scanner

The slice increment determines how much the gantry moves forward each circle and if it is shorter than the slice thickness, overlapping occurs, thus increasing the quality of the slices. This imaging protocol allowed an accurate 3D reconstruction of the femur from the iliac crest to the middle of the diaphyseal femur. (Fig 2.2)

Fig. 2.2: Coronal view of a CT-image showing the scanned region

2.1.3 CT calibration

Prior to the study, in order to get the mathematical relationship between HU of pixels and BMD (g/cm^3), the CT scan was calibrated with Quasar Phantom [45], enclosing different materials. The resultant of the calibration can be seen in the figure below (Fig. 2.3):
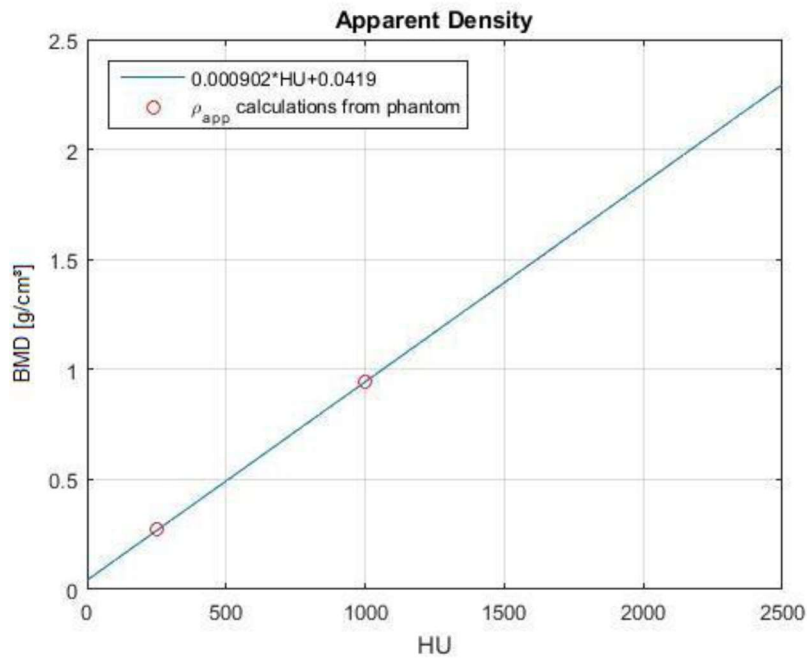

Fig. 2.3: BMD vs. HU relationship

Here instead the resulting formula [2.1]:

$$BMD \left[\frac{g}{cm^3}\right] = 0.000902 HU + 0.0419 \qquad [2.1]$$

2.1.4 Metal artefact reduction

Due to the presence of the prosthesis, the Post24 and Post1y dataset is strongly affected by metal artefact. The streaks derived from the implant change the HU of pixels of normal body tissue. In some cases, this artefact can significantly alter the values in the region of interest involved in this study. For this reason, the images are processed with the software *Metal Deletion Technique* from ReVision Radiology [46].

As explained in [47], the Metal Detect Technique (MDT) discards the inaccurate metal data and only uses the good quality ones to reconstruct the non-metal portion of the image. This process iteratively performs forward projection to replace detector measurements that involve metal. The result of MDT is shown in the figure below (Fig. 2.4).
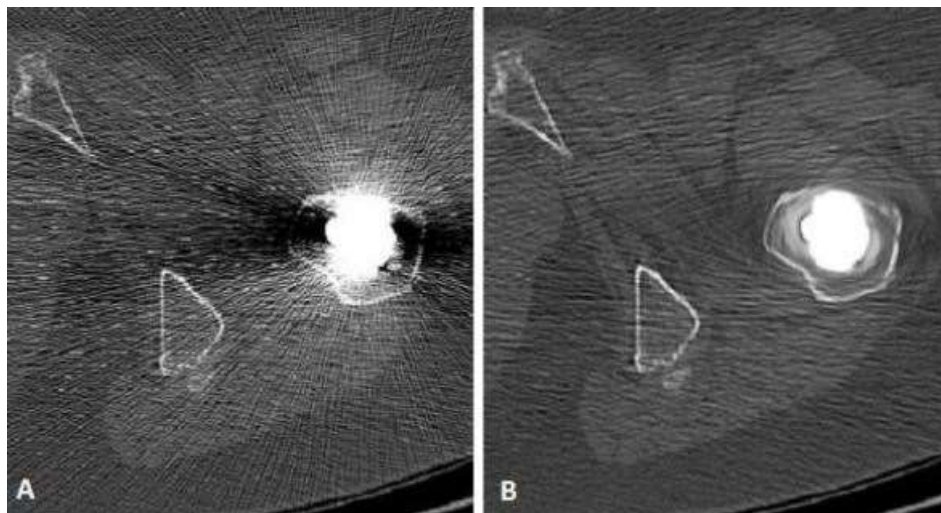

Fig. 2.4: Shows the same dataset before (A) and after (B) the artifact reduction process

2.2 3D Gain/Loss assessment

In this section, a method for the 3D evaluation of BMD changes is described. The protocol provides qualitative and quantitative information about gain and loss in patient undergoing THR, 1 year after the surgical operation. This protocol is applied to all the 8 uncemented patients and, for the first time, to 3 subjects with cemented fixation.
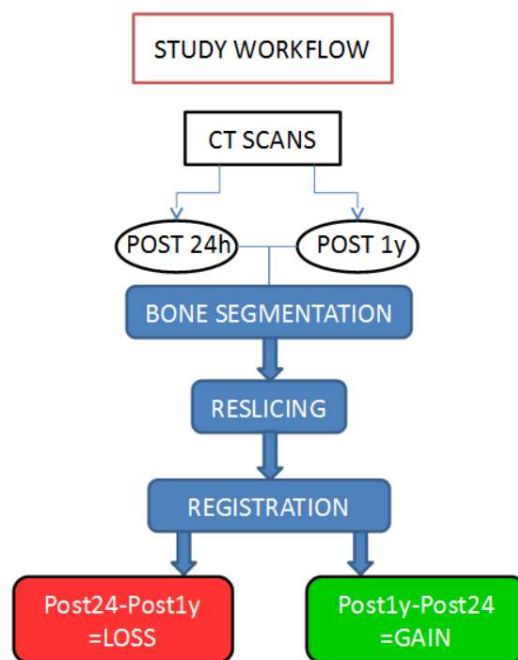
2.2.1 Study Workflow

Fig. 2.5 Study Workflow

The assessment methods are based on CT-scans acquired from patients undergoing THR at 3 different times: before operation, post 24 hours and 1 year post operation. The post 24 hours and the post 1 year images are processed, reconstructed in 3D, registered and compared; this way, the 3D evaluation of gain and loss after 1 year from THR is achieved. The same data are used, through a selection of standard slices, to implement the 2D approach.

2.2.2 Bone segmentation

In the 3D gain/loss protocol, the bone mask (set of pixels selected on the image) is obtained by a semi-automatic process.

After importing the CT-scan in Mimics®, performing segmentation, it is possible to separate the real bone from other tissues. This step is fundamental for the workflow, cause the analyses will involve this mask.

The "3D Live Wire" segmentation tool uses contour lines to manually follow the femur in the images. This is done every 5 to 10 slices depending on how the bone appeared, in both sagittal and coronal planes. The result of this could be reviewed in the axial plane before the segmentation. (Fig 2.6)
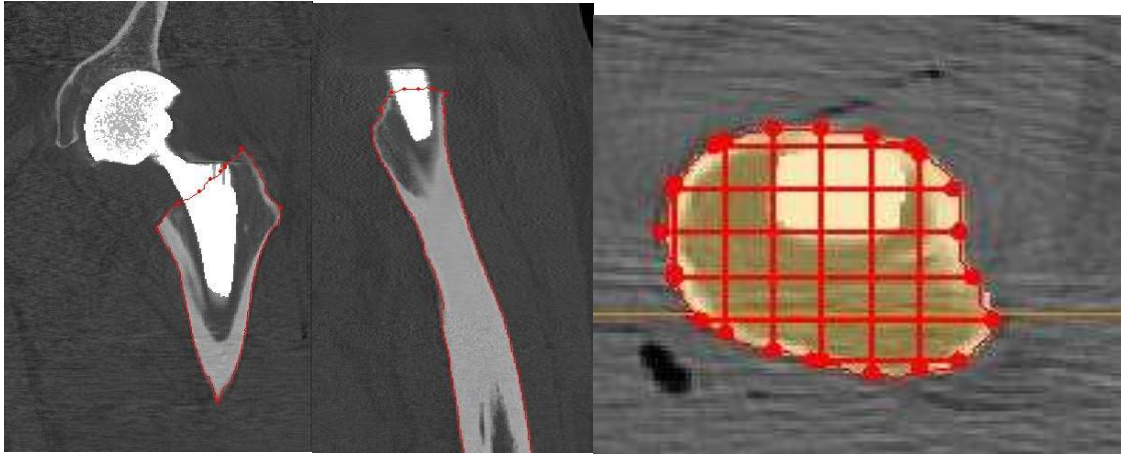

Fig. 2.6: The 3D Live Wire Tool workflow. First, contour lines were manually added between 5 to 10 slices in coronal and sagittal view. Contours were reviewed in the axial view. After that, the tool segmented the femur.

Then, 4 pixels are eroded from the bone mask.

A Boolean operation (Minus) between the bone mask and the eroded one, allow to have a "shell" that, basing upon previous studies, represents the external layer of the compact bone [48].

Separately, another mask is created through a threshold on the HU. In particular, 255 HU is set as the lowest value for the cancellous bone, while 3070 is considered as the highest value for the cortical bone.

This mask is then added (Boolean operation: Unite) to the "shell", thus having a unique mask in which apply the gain/loss evaluation, called "contour".

Using a unique threshold (3071 HU), the prosthesis is also segmented. A Boolean operation (Minus) is applied to the contour mask in order to separate the bone from the implant. (Fig. 2.7)

Finally, additional manual fine tuning is done to get rid of artifacts, e.g. due to stem's metal.

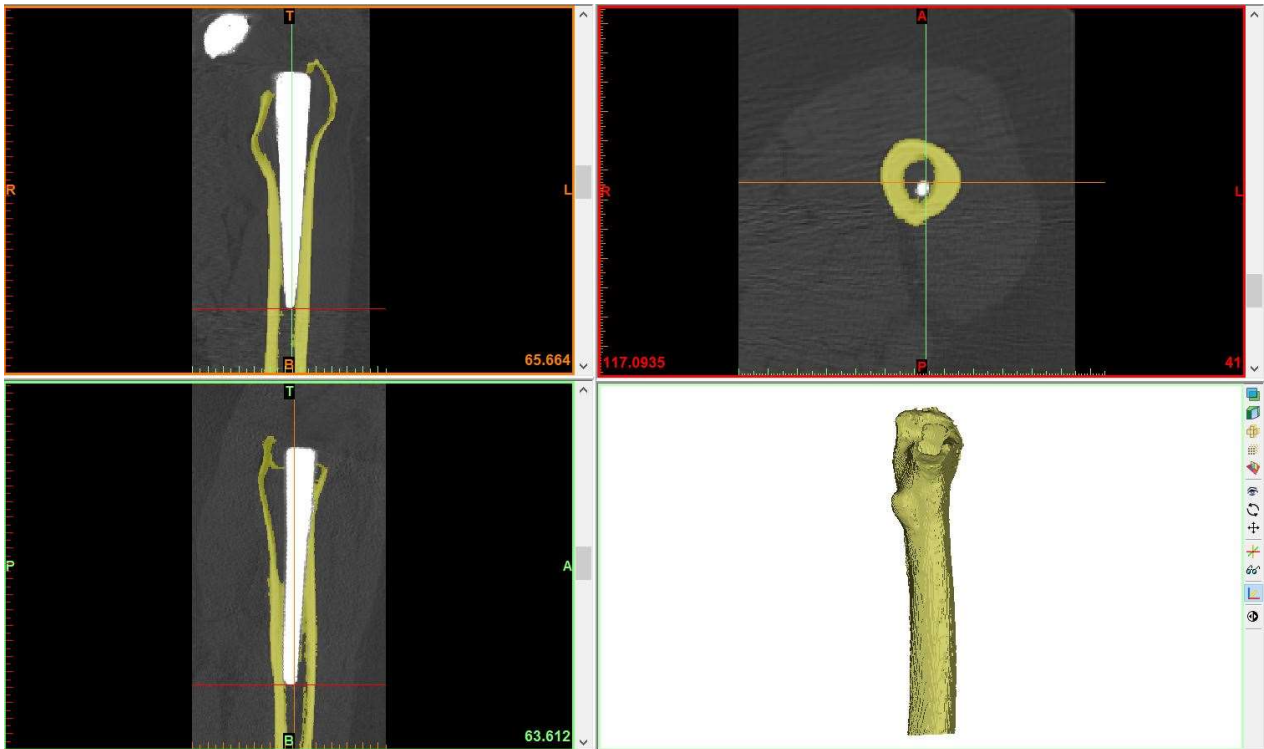The same process is repeated both for Post24 and Post1y dataset.

Fig. 2.7: 3D model of contour mask as result of the segmentation

2.2.3 Reslicing

Image registration is needed to align the two datasets so that the femur is in identical position between the scans. Anyway, although CT scanner machine and its settings are the same during the acquisitions (Post24 and Post1y), patient's lower limb can be rotated with different angles, thus complicating the assessment of gain/loss in the corresponding areas of the bone.

Through the Reslice Project Mimics it is possible to align the orientation of the body to have a better images registration. Moreover, with this step, pixel size of the two images is uniformed, since it is possible to define it during reslicing. Through a similar process, both Post 24h and Post 1y are resliced following a common line, in this case the longitudinal axis of the stem, which can be selected in the coronal view. Pixel size modification is applied to one of the two images, namely that with the highest value (lowest resolution). Its pixel value is modified setting it to other image's one, i.e. to the lowest value (highest resolution). Reslicing is also important to crop the area of interest of the femur, i.e. the proximal part, from the whole image for an easier analysis. (Fig. 2.8)
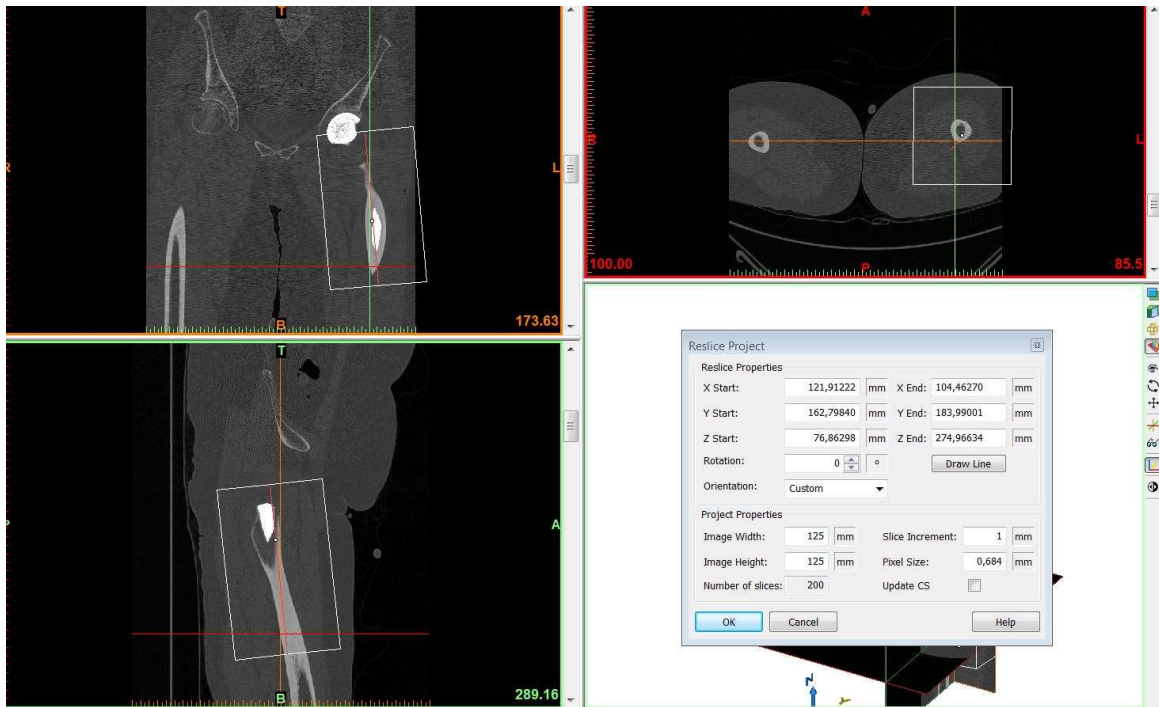
Fig. 2.8: Reslicing procedure

2.2.4. Image Registration

As already mentioned, for a correct evaluation of BMD changes, the 2 datasets need to be registered to compare the same zones of the bone.

In Mimics, a point-based registration is available to overlay the CT-scans, so this process is carried out identifying 6 points belonging either to the femur or the stem and considering anatomical landmarks which are easily recognizable (Fig. 2.9). These reference spots are:

a) Stem´s tip

b) Protuberance under greater trochanter (distal end of the attachment site for gluteus minimus)

c) Top of greater trochanter

d) Lesser trochanter

e) Gluteal tuberosity in axial view

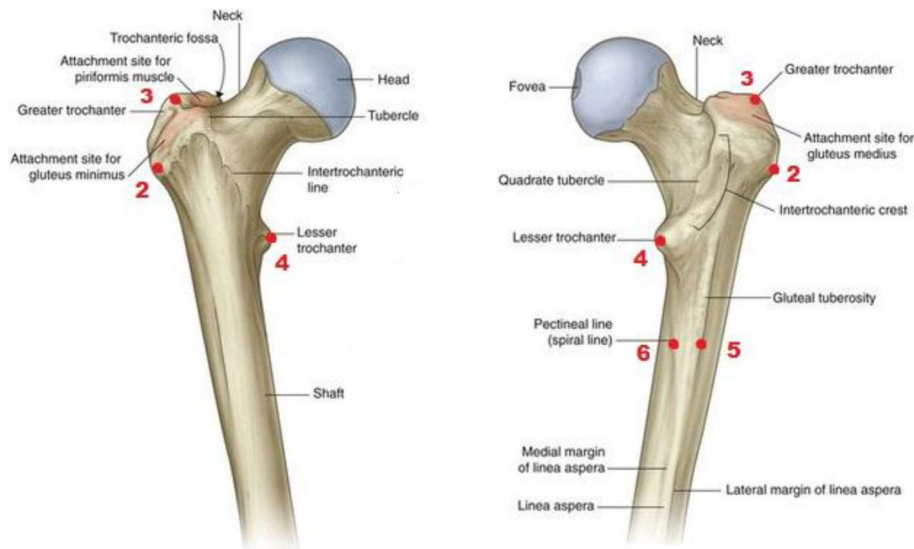f) Protuberance of pectineal line in axial view

Fig. 2.9: Landmarks for point-based Registration

Additionally, it is possible to add more landmarks to improve this procedure, although it is strongly recommended to use points belonging to the femur and not to the prosthesis or pelvis bone (except for suggested landmark a).

In the Image Registration tool, the Subtract Fusion Method is then selected. This way, while the scans are registered, a voxel by voxel intensity subtraction is performed. As result, a new Mimics project is created in which the GVr (resultant GrayValue) of a generic voxel is obtained by the difference between the GV of the correspondent voxels in the 2 datasets (GV_1-GV_2).

Since Mimics' Subtract Fusion Method sets to "black" (GVr = 0) all the voxels with either negative or null GVr, assigning a certain level of gray only if GVr is positive, one registration + subtraction procedure is made to evaluate bone gain, while the other one is made for bone loss. (Table 2.2)

DATASET 1	FUSION METHOD	DATASET 2	RESULT
1 y	Subtract	24 h	GAIN
24 h	Subtract	1 y	LOSS

Table 2.2: Subtract Method

2.2.5. Bone Gain/Loss evaluation

Once that the registration is complete, gain and loss in the femur are evaluated both quantitatively and qualitatively. The below-described steps are separately applied to each new Mimics Project, therefore bone resorption and bone growth are independently evaluated (as explained in Table 2.1).

First of all, the masks of the Post 24h and Post 1y femurs are imported (see § 2.2.2) in order to consider just the interesting pixels belonging to the bone.

The main source of error affecting a precise BMD changes assessment is the misalignment between the two registered datasets. A solution to this problem is to erode 3 pixels from the imported bone masks. This way, part of the outer femur is not considered in the comparison between Post 24h and Post 1y bone mineral densities.

Moreover, to examine significant BMD change only, a Threshold Mask is created having 111 GV as lower limit, according to the previous protocol. This corresponds to the minimum significant value of BMD change, meaning that a GVr loss (or equivalently a GVr gain) lower than 111 is not considered to be relevant.

Successively, by doing a Boolean operation of Intersection between the Eroded Femur Mask and the Threshold Mask, the Final Loss (or Gain) Mask is achieved.

Checking the mask properties, information about the volume (mm3) of bone lost (or gained) is obtained, along with the volume of the femur mask. This way it is possible to calculate the percentage of lost and gained volume 1 year after THR using the following formulas [2.2, 2.3]:

$$\% \, Loss = \frac{Mask \, Volume \, Loss}{Mask \, Volume \, Femur \, Post24} \times 100 \qquad [2.2]$$

$$\% \, Gain = \frac{Mask \, Volume \, Gain}{Mask \, Volume \, Femur \, Post1y} \times 100 \qquad [2.3]$$

Finally, a three-dimensional representation of the loss/gain areas over the proximal femur is realized, to better understand where the changes have occurred.
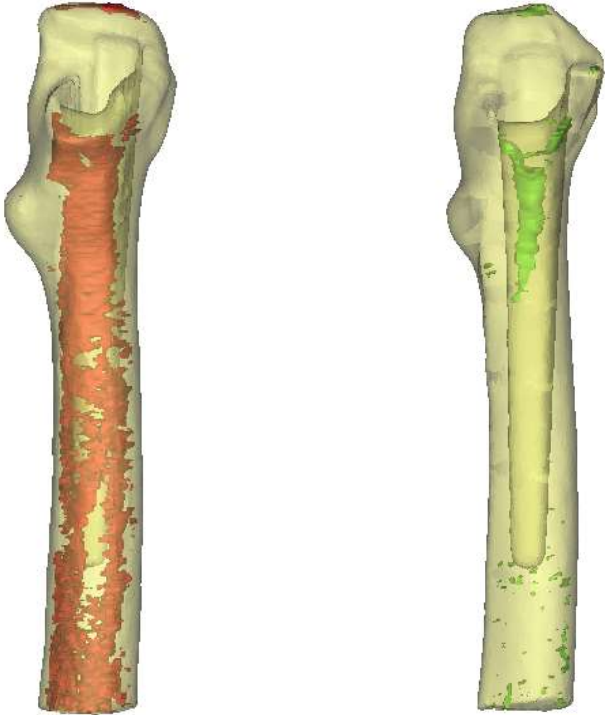

Fig. 2.10: Results of the 3D assessment for patient #1. Loss (Red) and Gain (Green)

2.3 Cross-section based assessment

In order to define an ethically compatible method to assess bone condition, two different procedures are described, based on the selection of 5 standard CT-scans. The first one utilizes Matlab Image Processing Tool to obtain information about gain and loss in single slices. The second one instead aims to introduce a strong method to extract a distribution (HU values-N° of pixels) from the image which can be used to study bone quality.

2.3.1 Selection of standard CT-scans

Cause standard cross-sectional slices are needed to apply the 2D approach, five CT-scans were selected from the dataset, according to the work of Pitto et al. [49]. Listed from the most proximal to the most distal, the 5 regions of interest are: 1) greater trochanter; 2) lesser trochanter; 3) 5 cm proximal to stem's tip; 4) stem's tip; 5) 2 cm distal to stem's tip. (Fig. 2.11)
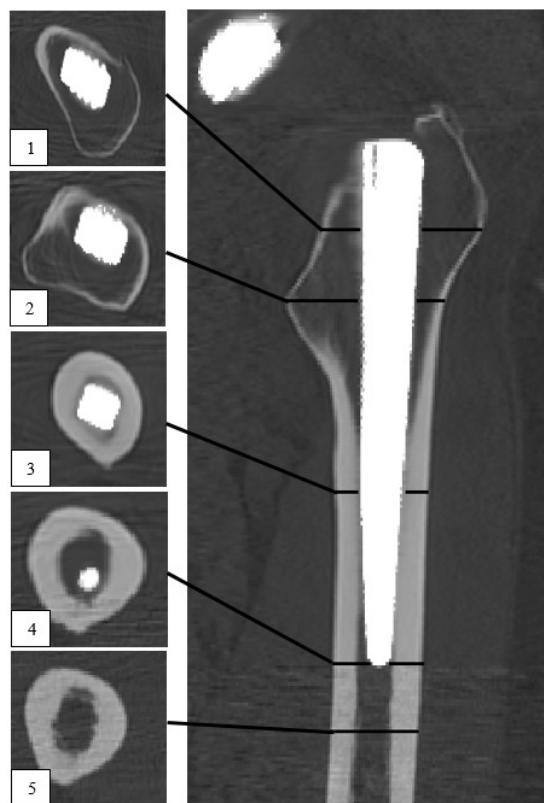

Fig. 2.11: 5 Regions of Interest for BMD: 1) Greater Trochanter, 1) Lesser Trochanter, 3) 5 cm proximal to stem's tip, 4) stem's tip, 5) 2 cm distal to stem's tip. F) Coronal view.

These CT-scans have been chosen also because they are easily detectable in both Post24 and Post1y dataset. Moreover, these slices define 5 volumes of interest in which BMD changes can be evaluated

by the 3D assessment (using formulas [2.2, 2.3]), providing interesting information on how the gain and loss is distributed in each sub-volume. (Fig. 2.12)
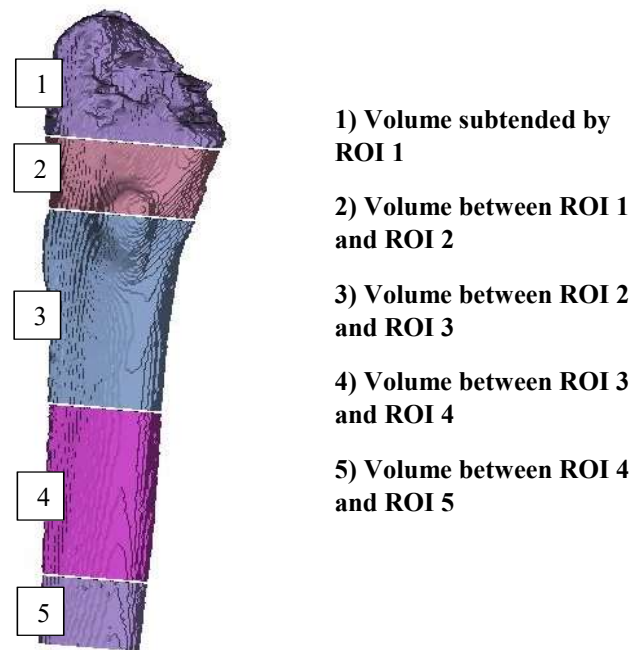

1) Volume subtended by ROI 1

2) Volume between ROI 1 and ROI 2

3) Volume between ROI 2 and ROI 3

4) Volume between ROI 3 and ROI 4

5) Volume between ROI 4 and ROI 5

Fig. 2.12: 5 sub-volumes of the 3D femur

2.3.2 Gain/Loss assessment using Matlab Image Processing Toolbox

In this paragraph, pursuing the same target of the 3D gain/loss analysis, a new approach based on the registration of 2 slices of the same ROI is presented. Following the workflow described in §2.2.1, an alternative procedure has been developed in Matlab to evaluate the formation and erosion of bone in single images.

The selected CT-scans (see §2.3.1) can be imported as DICOM format and then it is possible to apply an algorithm of automatic registration [50] to overlay the images and reproduce the 3D gain/loss assessment.

Starting from the same segmentation performed in MIMICS, the contour mask is also imported along with the slices. Instead of doing the registration considering all the image, the mask is firstly used to separate the bone from other tissues and then the automatic algorithm is applied, thus having a better alignment of the scans.

As explained §2.2.5, a similar erosion of the outer layer of the femur is carried out (2 pixels eroded), as well as the utilization of the same threshold on GV.

Finally, using formulas [2.2, 2.3] the percentage of gain and loss in the slice is calculated.

31

The main steps of the Intensity Based Algorithm are shown in the scheme below (Fig. 2.13).
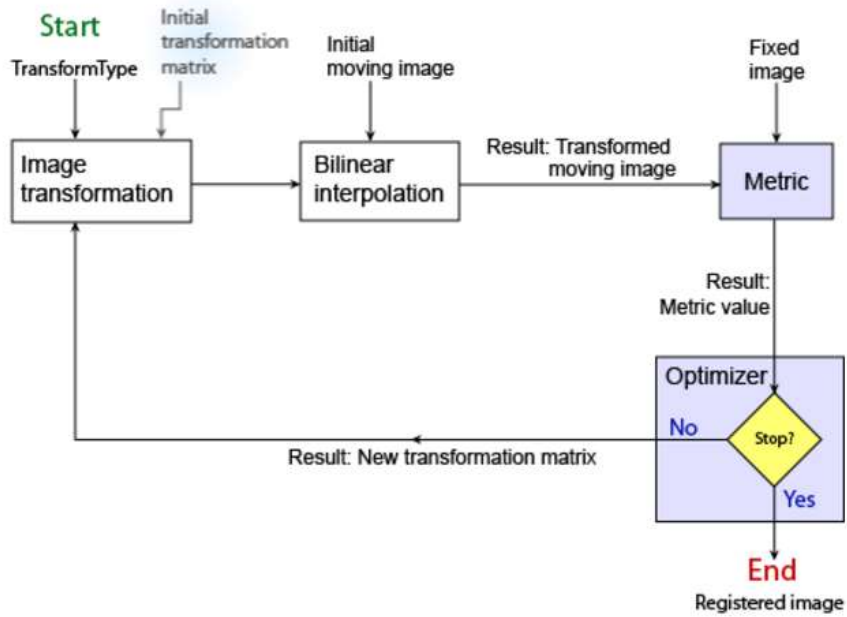

Fig. 2.13: Intensity Based Algorithm workflow (from [51])

The fundamental principle of intensity-based procedures is to look for, in a defined space of transformations, the one that maximizes (or minimizes) a criterion measuring the intensity similarity of corresponding voxels. Some measures of similarity are based on squared differences in pixel intensities, regional correction, or mutual information [52]. Having a 'monomodal' registration (CT-scans taken in different times), Matlab algorithm performs a series of iterations to minimize the mean squares between the images, computed by squaring the difference of corresponding pixels in each slice and considering the mean of those squared differences.
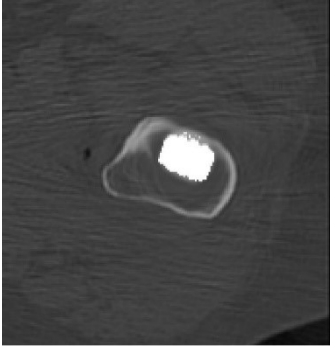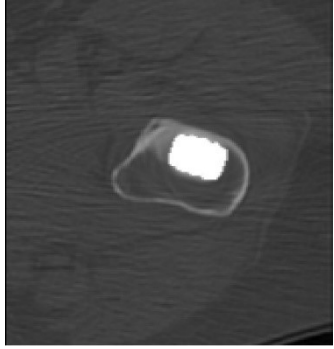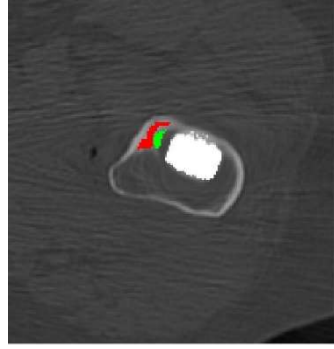
Region of Interest	Slice Post24	Slice Post1y	Gain/Loss
ROI 2			

Fig 2.14. Result of Image Registration for ROI 2 of patient #1

2.3.3 2D bone-profile analysis

Starting from the same bone mask created for the 3D approach, it is possible to export the HU of the pixels belonging to these slices and then examine, trough Matlab software, the density distribution Similar analysis was used in other works to study the distribution all over the femur (Fig. 2.15: the peak corresponding to lower HU values the cancellous bone, the second peak corresponding to higher HU is the cortical bone). The novelty of this thesis is represented by the fact that the focus is just on standard single CT-scans.
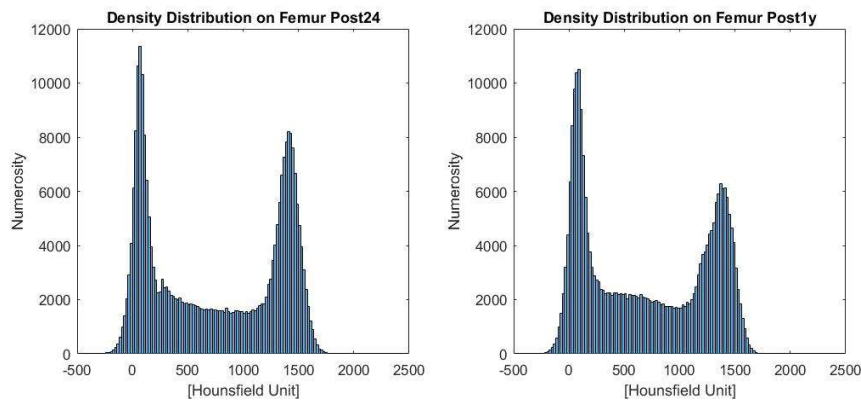

Fig. 2.15: Density Distribution over the mask of the operated femur's 3D model: Post24 and Post1y dataset

Based upon other studies in which 2D evaluation involved the density distribution of segmented muscles [53], a histogram was made for each slice showing the number of pixels belonging to a certain interval of Hounsfield unit values and hence the bone profile at the time of the scan.

It is evident that a change in the distribution, comparing Post24 and Post1y data of the same ROI, can offer some information about the mechanism of bone remodeling. Therefore, the main goal of this studies is to find a good model to fit the profile and extract some parameters that can be used to evaluate bone quality or BMD gain/loss.

2.3.4 Model Fitting

After importing the slice mask in Matlab (coordinates of pixel and HU), a qualitatively evaluation of the distribution is made.

Concerning the ROI 3-4-5, the CT-scans show that the cortical bone is predominant in the diaphyseal femur, with only few pixels of cancellous bone. Part of the slice includes other tissues (like bone marrow) that are not interesting for the assessment. For this reason, it is decided to take only the pixels with an HU between 255 and 2500. The lower limit is the same of the 3D procedure, while the upper one has been chosen looking at the highest HU value of the set of distributions investigated.

On the contrary, ROI 1-2 are principally composed by cancellous bone, with only a thin layer of compact bone. In this case, to not lose information on trabecular bone, the lower limit is set to -500 HU, having the same higher limit (2500 HU).

Since the analysis involves just single slices, with a very low number of pixels, some considerations are done about the histogram. In the first place, it is decided to divide the entire range of values from the lower limit to 2500 HU in a series of interval of 10 HU (*bin*). This means that the histogram counts how many pixels fall into these subintervals to define the profile. A shorter bin is incompatible with a good fitting, cause the number of pixels is insufficient to cover all the range of Hounsfield unit values (the result is a histogram with lot of 0 values for the bin with no pixels in it). On the other hand, a bigger bin can lead to a low sensitivity in the discretization of pixels' values, thus having a not significant distribution.

Moreover, following the pre-processing steps used for the analysis of muscles' quality, the distribution is "smoothed" with a digital filter. This operation clearly generates a loss of information (especially in the peak of each tissue), but it allows a better model, based upon the value of R^2.

As already mentioned, the fitting of the radio-densitometric HU distributions is adapted from a previous regression analysis methodology utilized on CT scans of lower limbs to measure changes in muscle quality [54].

First, it is important to define any distribution of tissue of a given radio-density as based on a standard Gaussian distribution. The main hypothesis is that the distribution of HU values correlating to that tissue varies according to a normal probability density function described by the equation below:

$$\varphi(x, \mu, \sigma, N) = \frac{N}{\sigma\sqrt{2\pi}} e^{-\frac{(x-\mu)^2}{2\sigma^2}}$$
[2.4]

where φ represents the probability density function of the tissue type, N is the Gaussian distribution's relative amplitude, μ is the location of the distribution's mean, and σ is the width of the distribution – all of which may be evaluated as a function of each pixel or voxel's computed HU value (variable *x*).

To simplify the model fitting, the equation is modified as follow:

$$\varphi(x, \mu, \sigma, A) = Ae^{-\frac{(x-\mu)^2}{2\sigma^2}}$$
[2.5]

in the new formulation, the parameter A assumes exactly the value of the amplitude of the distribution (number of pixels with a HU equal to the mean value μ).

Cause different tissues are present in the slice, the optimum regression analysis needs the definition of a generalized tissue distribution function that contains each of the tissue types. Writing this in simple notation that sums the Gaussians:

$$\sum_{i=1}^{m} \varphi(x, \mu_i, \sigma_i, A_i) = A_i e^{-\frac{(x-\mu_i)^2}{2\sigma_i^2}}$$
[2.6]

where *m* is the number of Gaussians considered in the fitting and depending on profile's shape.

This way, in Matlab, using regression analysis, it is possible to find the best fitting for the distribution. To perform this, the software employs an iterative generalized reduced gradient algorithm through the minimization of the sum of standard error. After running hundreds of iterations, the standard error at each point is gradually and progressively reduced. At the end, it is possible to compute the R^2 value for the theoretical curve's fit to the image data starting from the sum of all standard errors. This procedure uses the following set of equations:

$$R^2 = 1 - \frac{SSE}{SST}, \quad SST = \sum_{i=1}^{n}(y_i - \bar{y})^2, \quad SSE = \sum_{i=1}^{n}(y_i - f(x_i))^2$$

[2.7]   [2.8]   [2.9]

where:

-*n* is the number of data points;

-SST is the "total sum of squares" and quantifies how much the data points, y_i vary around their mean $\bar{y}$.

-SSE is the "error sum of squares" and quantifies how much the data points, y_i, vary around the modeled values, $f(x_i)$.

In sum, the above procedure provides a unique HU distribution equation for each image which is defined by its own parameters. These distributions parameters may then be exported for a series of analyses and comparison.
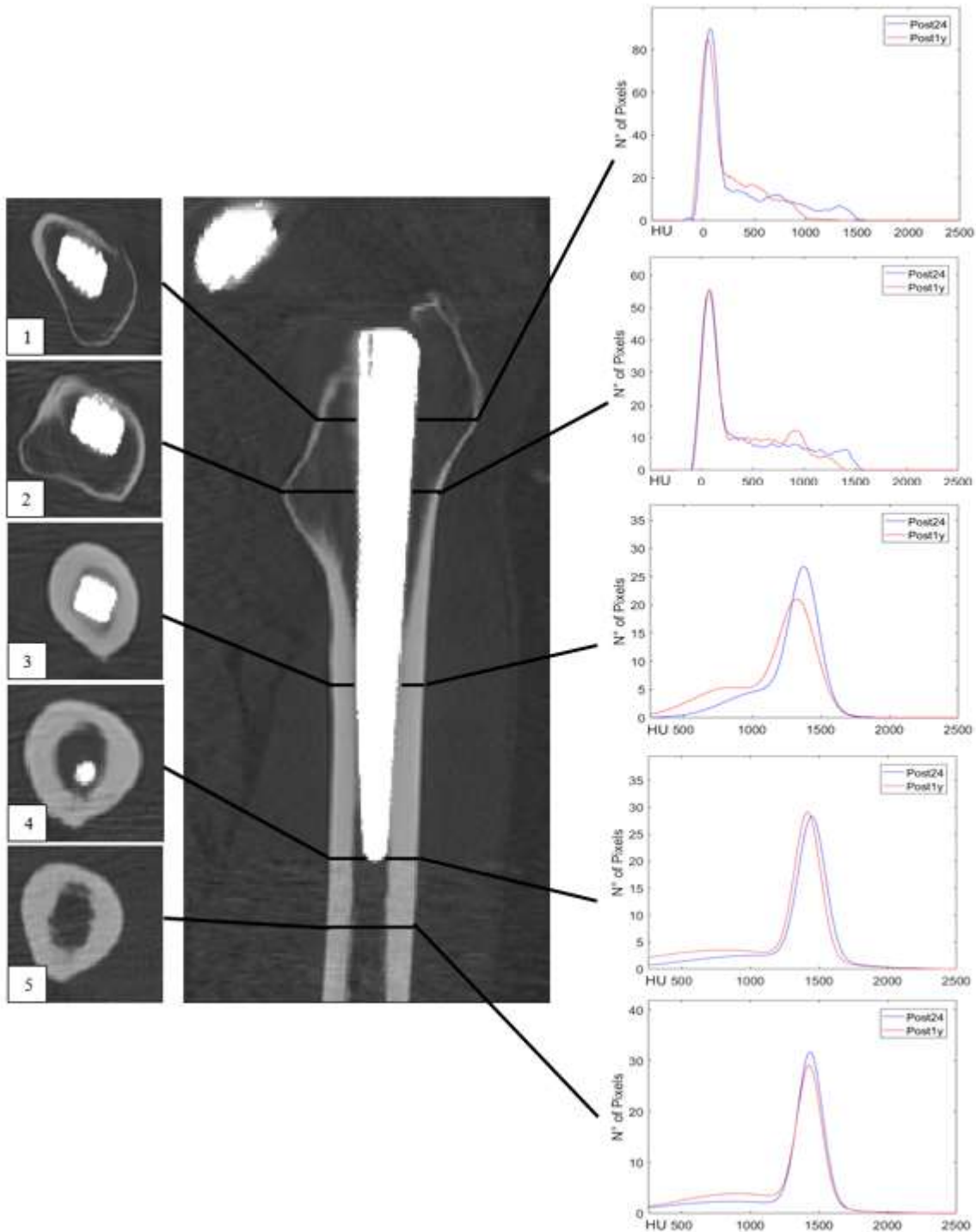

Fig. 2.16. Comparison Bone Profile (Post24-Post1y) for the 5 ROI in patient #1: note that for ROI 1 and 2 the fitting is not performed.

3. Results

In this section, the main outcomes of this work are presented. The chapter is divided into two parts: in the first one, it is shown the analysis of the patients' dataset, resulting from the application of the new protocol for 3D gain/loss evaluation. In the second one instead, the focus is on the cross-section based assessment.

3.1 3D Gain/Loss assessment

3.1.1 Comparison between protocols

Outcomes of the new protocol (protocol 2) are compared to the previous one (protocol 1; [55]). Through the semi-automatic process of segmentation explained in § 2.2.2, the 3D assessment shows an improvement in terms of sensitivity in the gain/loss evaluation. In fact, due the low quality of CT-scans and to the BMD differences between subjects, a segmentation performed solely with a threshold on the HU can lead to the creation of a contour mask with holes and lack of information, thus influencing the results, while the new process allows a better rendering of the 3D model (Table 3.1).
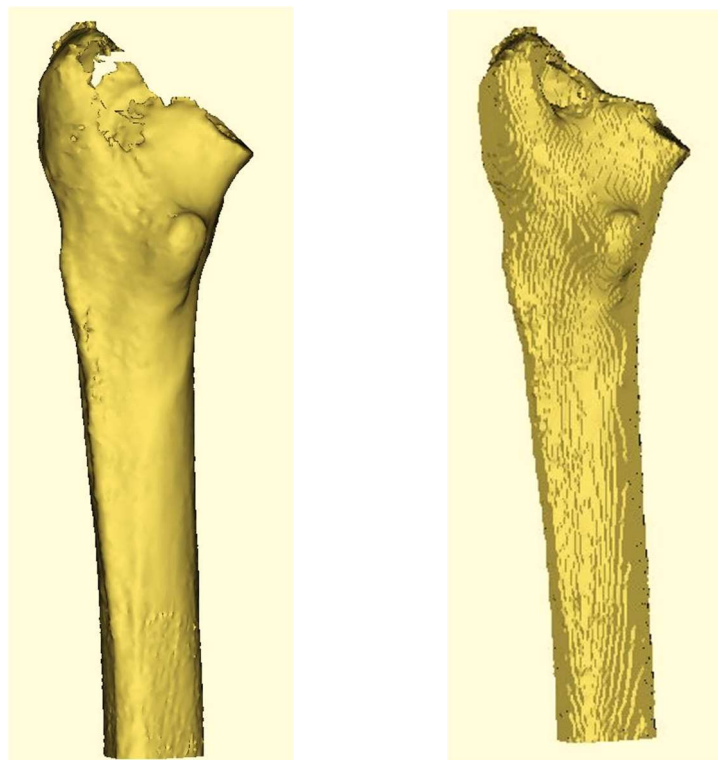

Fig. 3.1: 3D Contour Mask: protocol 1 (left); protocol 2 (right)

✅	**3D Model Rendering**	The new process allows a better rendering of the 3D model. (Fig 3.1)
✅	**Augmented Gain/Loss sensitivity**	The mask volumes for loss and gain are greater in the protocol 2, cause more bone is considered during the evaluation. (Table 3.2, 3.3)
✅	**Less affected by thresholding operation**	The thresholds used in protocol 1, can lead to discard pixels that correspond to bone tissue. With the semi-automatic segmentation, it is possible to manually select the bone of the outer layer of the femur.
✅	**Assessment for cemented dataset (poor quality image)**	Protocol 2 can be used to analyze cemented dataset.
❌	**Less automatic process**	Evaluation based on a manually segmentation of the bone.

Table 3.1: Protocol 2, features

Below, a comparison between the 2 protocols is carried out for 3 patients, showing the volume of the mask (mm^3) used to compute the percentages of gain and loss. (Table 3.2, 3.3)

Patient	AGE	Gender	CONTOUR VOLUME Protocol 1 (mm^3)	LOSS VOLUME Protocol 1 (mm^3)	LOSS Protocol 1 %	CONTOUR VOLUME Protocol 2 (mm3)	LOSS VOLUME Protocol 2 (mm3)	LOSS Protocol 2 %
UNCEM	60	F	87967.9	4995.4	5.7	105667.2	6691.2	6.3
UNCEM	54	F	98873.7	5699.1	5.8	115556.9	6947.2	6.0
UNCEM	60	M	139201.4	2917.9	2.1	153419.6	3357.9	2.2

Table 3.2: Loss assessment, comparison between protocols

Patient	AGE	Gender	CONTOUR VOLUME Protocol 1 (mm^3)	GAIN VOLUME Protocol 1 (mm^3)	GAIN Protocol 1 %	CONTOUR VOLUME Protocol 2 (mm^3)	GAIN VOLUME Protocol 2 (mm^3)	GAIN Protocol 2 %
UNCEM	60	F	88928.5	784.0	0.9	96309.0	837.8	0.9
UNCEM	54	F	110403.4	2610.7	2.4	118415.2	2882.4	2.4
UNCEM	60	M	138427.9	814.4	0.6	151098.5	1062.1	0.7

Table 3.3: Gain assessment, comparison between protocols

The results highlight how the mask volumes for loss and gain are greater in the improved protocol, cause more bone is considered during the evaluation. This difference is also present in the final percentages of gain and loss, although sometimes is not significant cause to a bigger volume of BMD changes correspond also a bigger volume of the contour mask.

3.1.2 BMD changes: qualitatively comparison

Through the 3D assessment it is possible to have a volumetric description of BMD changes. This way, it is possible to qualitatively compare gain and loss in each patient, looking the 3D model of the femur and examining the areas in which the bone remodeling is stronger. (Fig. 3.2)

| F, 60, CEMENTED | F, 60, UNCEMENTED | F, 54, UNCEMENTED |
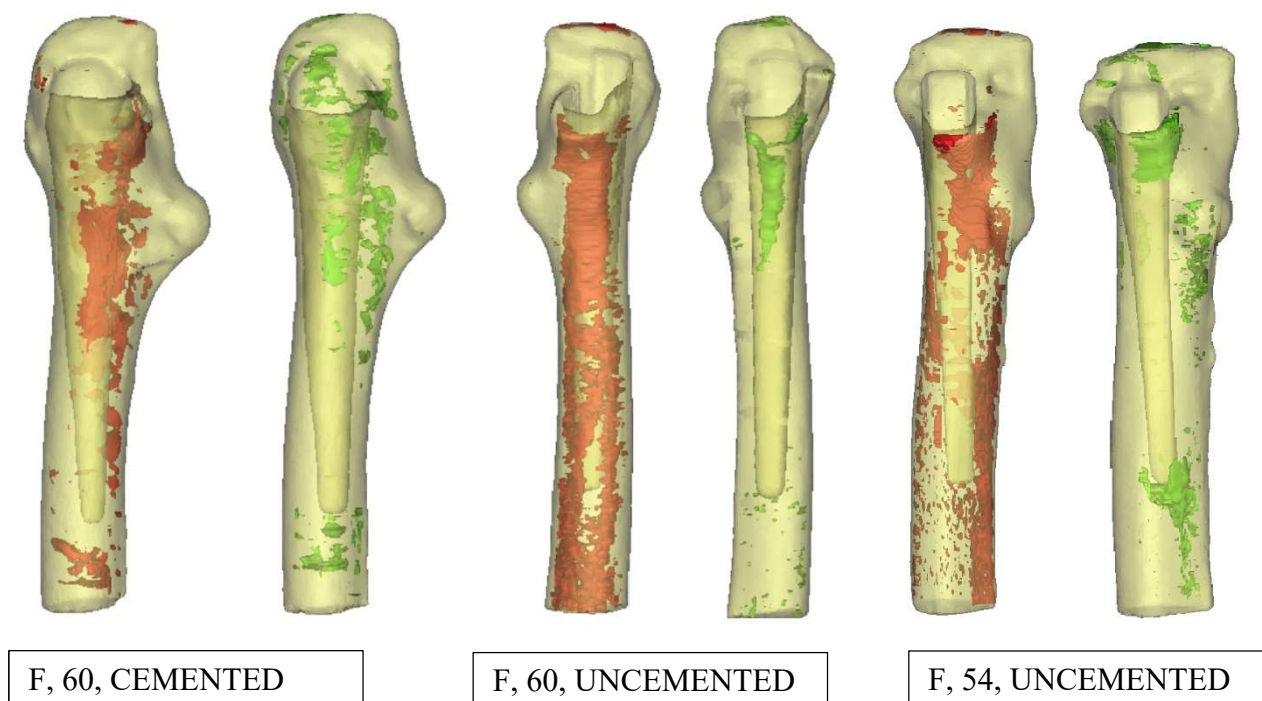
Fig. 3.2: 3D femur's model: Loss and Gain

The results show that the medial proximal area of the femur around the lesser trochanter is most susceptible of bone loss. Some bone gain can be seen at the various regions of the femur, mostly at the distal part.

For the sake of clarity, it is fair to point out that for cemented dataset just the proximal part of the femur is considered, down to 20 mm distally to stem's tip, due to a bad scan protocol (CT-scans started from less than 4 cm under the tip of the stem), while for the uncemented one the 3D femur is considered down to 40 mm distally to stem's tip.

3.1.3 BMD changes: volume fractions

The total dataset is composed by 11 patients: 8 received an uncemented implant, 3 a cemented one. To perform a quantitative comparison between the subject, percentages of gain and loss in the 5 volumes of interest (VOI), obtained with the crop of the entire femur mask, are measured.

Figures 3.3 and 3.4 report a summarize of percentages of gain and loss for all the patients.

Fig. 3.3: 3D Loss in 5 VOI
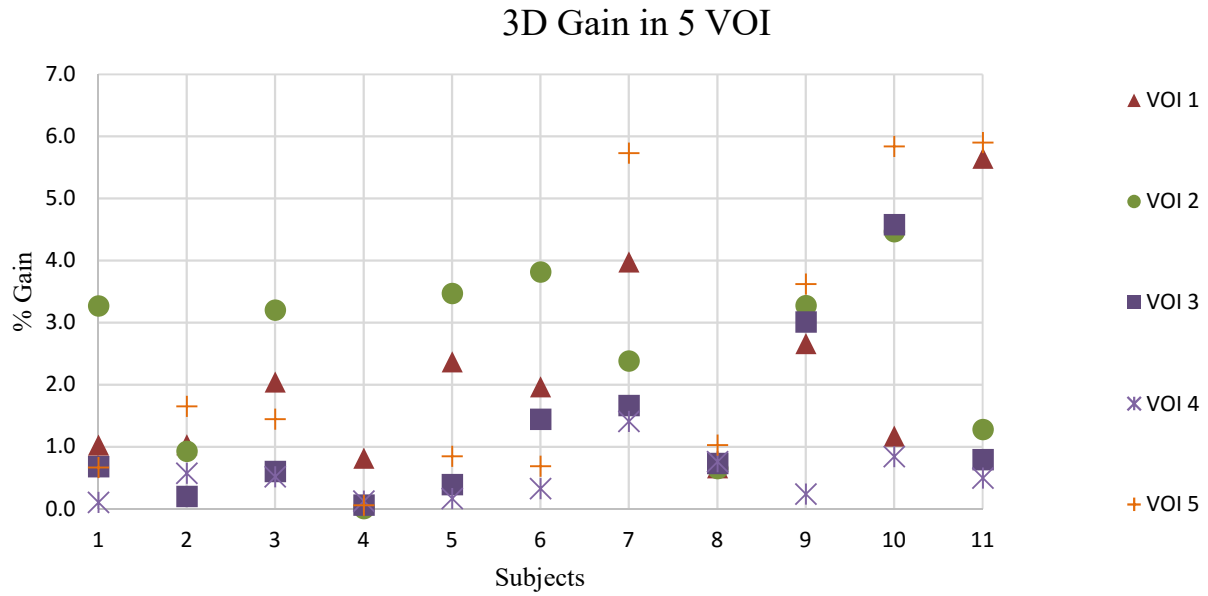
Fig. 3.4: 3D Gain in 5 VOI

The maximum loss is registered for patient 5 (uncemented) in region 3: 29.8 %. The minimum loss is in patient 8 (uncemented), in the regio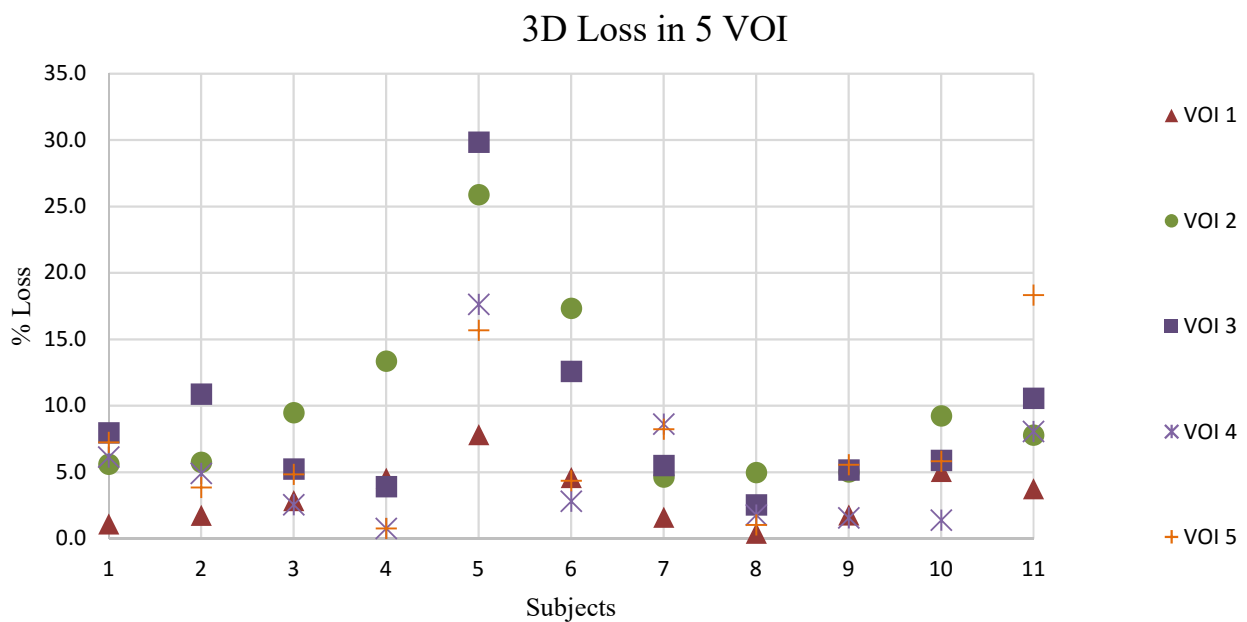n of greater trochanter: 0.4%. The maximum gain is registered for patient 11 (cemented) in region 5: 5.9%. The minimum gain appears in patients 4 (uncemented), 2 cm under the tip, having no change.

3.2 Cross-section based assessment
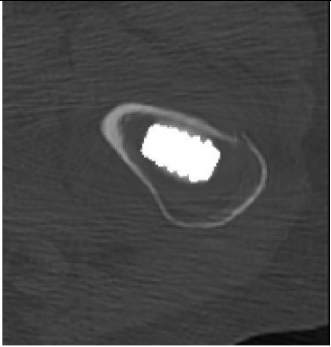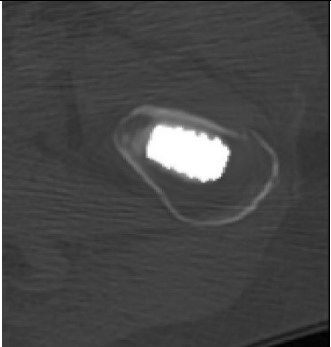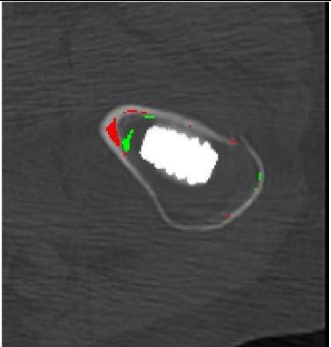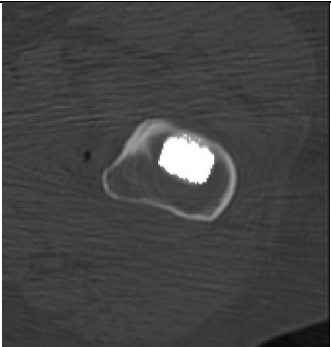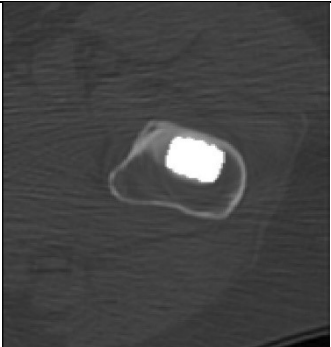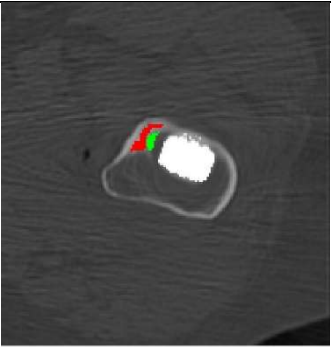
Below the main results of the cross-section based assessment are shown for 8 patient of the entire dataset (uncemented). Future analysis can involve a larger cohort of patients, including subjects with cemented implant.

3.2.1 Gain/Loss assessment using Matlab Image Processing Toolbox

The standard CT-scans selected from the Post24 and Post1y dataset have been registered through an automatic algorithm in Matlab to replicate the 3D evaluation. For each slice, the percentages of gain and loss are calculated, similarly to what has been done for the volumetric assessment. Moreover, the areas of BMD changes are evidenced in the Post24 image, thus having a qualitative description of the zones facing bone remodeling (as shown below for Patient #1).

- **Patient #1, F, 60**

    Image Registration Results:

Region of Interest	Slice Post24	Slice Post1y	Gain/Loss
Greater Trochanter			
Lesser Trochanter			

5 cm proximal to stem's tip			
Stem's tip			
2 cm distal to stem's tip			
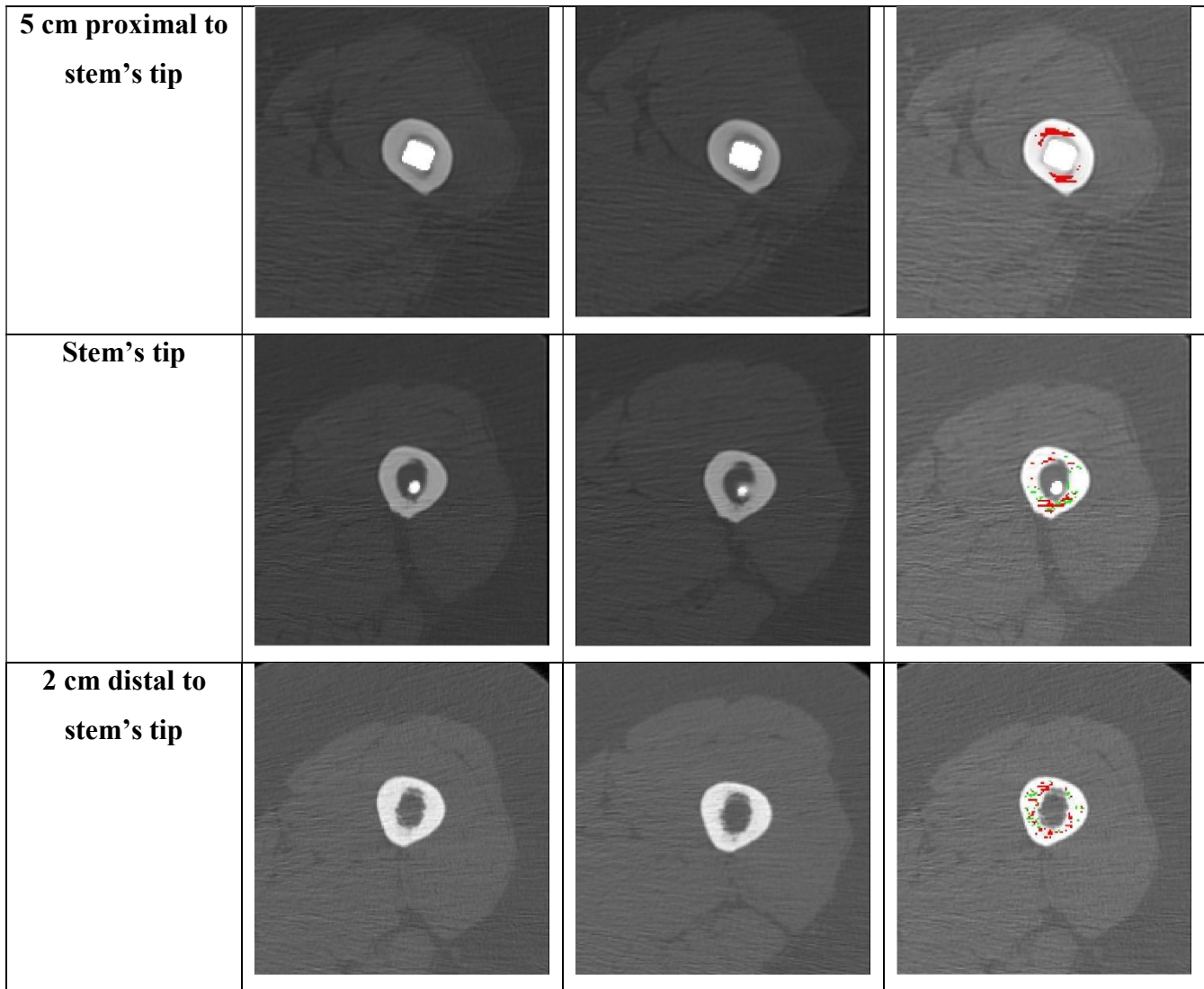
Percentages of Gain/Loss in the 5 slices (see § 2.3.1) are now presented for each patient, as output of the Matlab analysis.

- **Patient #1, F, 60**

Region	Loss%	Gain%
Greater Trochanter	5.6	2.9
Lesser Trochanter	8.4	3.3
5cm proximal to stem's tip	12.4	0.1
Stem's tip	7.8	3.8
2cm distal to stem's tip	8.8	3.5

- **Patient #2, F, 48**

Region	Loss%	Gain%
Greater Trochanter	13.3	5.5
Lesser Trochanter	10.7	2.6
5cm proximal to stem's tip	9.3	0.6
Stem's tip	4.9	5.2
2cm distal to stem's tip	10	8.9

- **Patient #3, M, 50**

Region	Loss%	Gain%
Greater Trochanter	13	4.1
Lesser Trochanter	14.5	4.1
5cm proximal to stem's tip	8.6	1.8
Stem's tip	4.7	2.3
2cm distal to stem's tip	6.7	6.9

- **Patient #4, F, 61**

Region	Loss%	Gain%
Greater Trochanter	18.4	1.1
Lesser Trochanter	9.1	1.7
5cm proximal to stem's tip	1.9	0.6
Stem's tip	0.7	0.9
2cm distal to stem's tip	5.3	0.2

- **Patient #5, M, 48**

Region	Loss%	Gain%
Greater Trochanter	15.5	0.6
Lesser Trochanter	22	2
5cm proximal to stem's tip	22.2	0.8
Stem's tip	13.8	0.3
2cm distal to stem's tip	19.7	1.6

- **Patient #6, M, 49**

Region	Loss%	Gain%
Greater Trochanter	19.8	5.9
Lesser Trochanter	27.3	9.1
5cm proximal to stem's tip	6.6	4.1
Stem's tip	6.9	2.6
2cm distal to stem's tip	15.9	5.4

- **Patient #7, F, 54**

Region	Loss%	Gain%
Greater Trochanter	11.2	9.8
Lesser Trochanter	7.7	1.4
5cm proximal to stem's tip	14.7	0.6
Stem's tip	16.8	15
2cm distal to stem's tip	15.2	3.3

- **Patient #8, M, 60**

Region	Loss%	Gain%
Greater Trochanter	8.1	0.9
Lesser Trochanter	6.2	0.5
5cm proximal to stem's tip	9.3	1.9
Stem's tip	2.7	4.3
2cm distal to stem's tip	6.6	2.4

3.2.2 2D Bone Profile

The Density Distribution (HU-n° of pixels) is used to assess bone quality in the 5 ROI. A series of parameters are extracted from the Gaussian Fitting and then compared to the BMD changes of the 3D approach, looking for a correlation.

Of the 5 slices selected in this work, only 3 offer a profile that can be fitted with the regression analysis. As described in § 2.3.4, the fundamental hypothesis is that the distribution of HU for each tissue (in this case: cortical bone and cancellous bone) vary according to a Gaussian function. For ROI 1 and ROI 2 (Greater Trochanter and Lesser Trochanter), probably due to the low number of pixels corresponding to the cortical bone, such hypothesis is not verified.

For this reason, the 2D profile analysis involves only ROI 3, 4, 5, in which the cortical bone is predominant and can be fitted with a Gaussian distribution, while a second Gaussian is used to model the few pixels with low HU (cancellous bone, low dense cortical bone, ...).

Therefore, for ROI 3, 4, 5, a bimodal fitting is chosen, generating for each slice a profile which is defined by its own 6-parameter: N, μ, σ for both cortical and cancellous bone. It is important to clear out that, for these regions, the analysis of the parameters involves only the Gaussian corresponding to the cortical peak. As shown in the CT-scans in fact, ROI 3, 4, 5 mostly consist of compact bone, so any change in bone quality can be correlated to a modification of the parameter of the first Gaussian.

To provide a measure of how well the theoretical curve fits the image data, as explained in § 2.3.4, the R^2 value is computed, defining a threshold ($R^2 > 0.96$) above which the fitting is considered good.

Below, the values of R^2 shown for the diaphyseal regions of interest: 5 cm proximal to stem's tip (ROI 3); stem's tip (ROI 4); 2 cm distal to stem's tip (ROI 5).
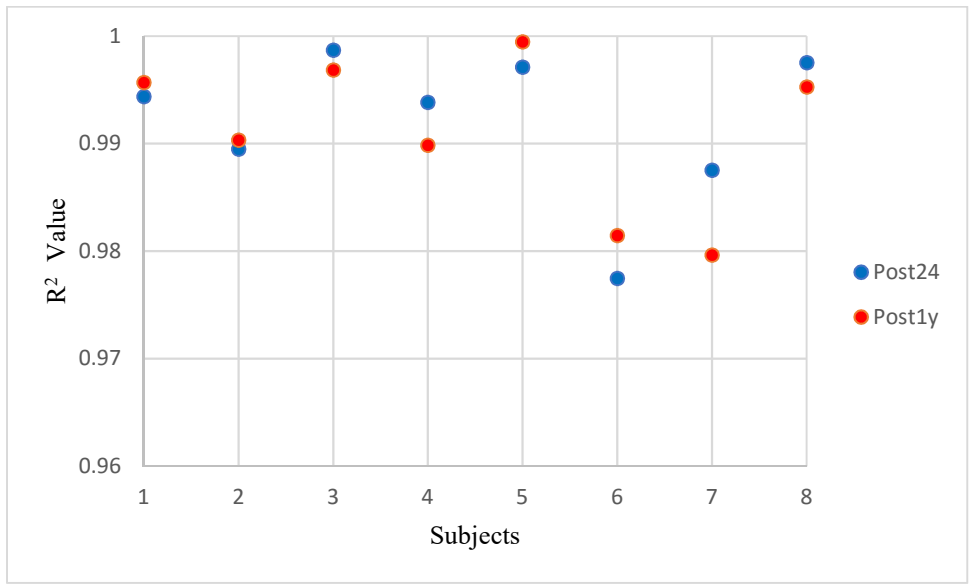
Fig. 3.5: R² values for ROI 3
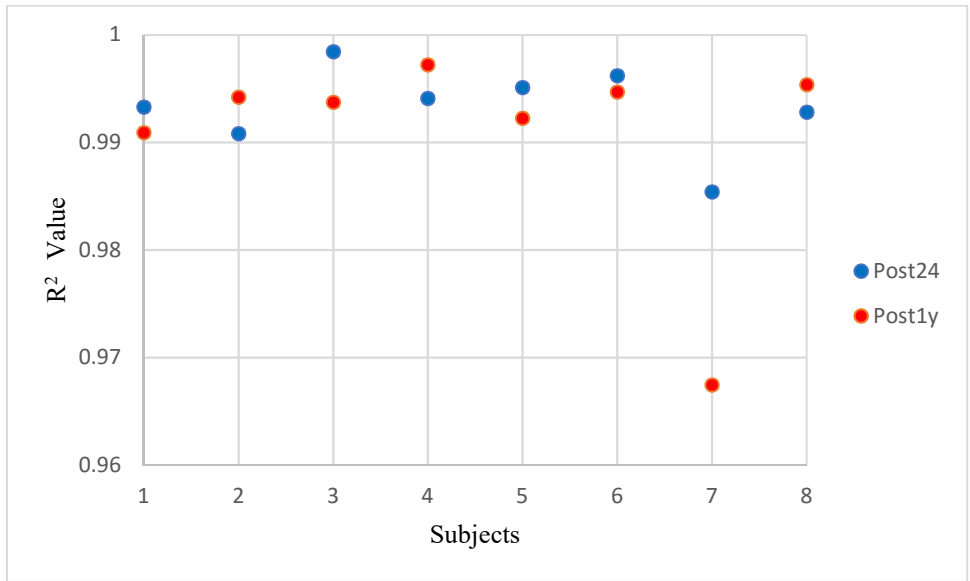
Fig. 3.6: R² values for ROI 4
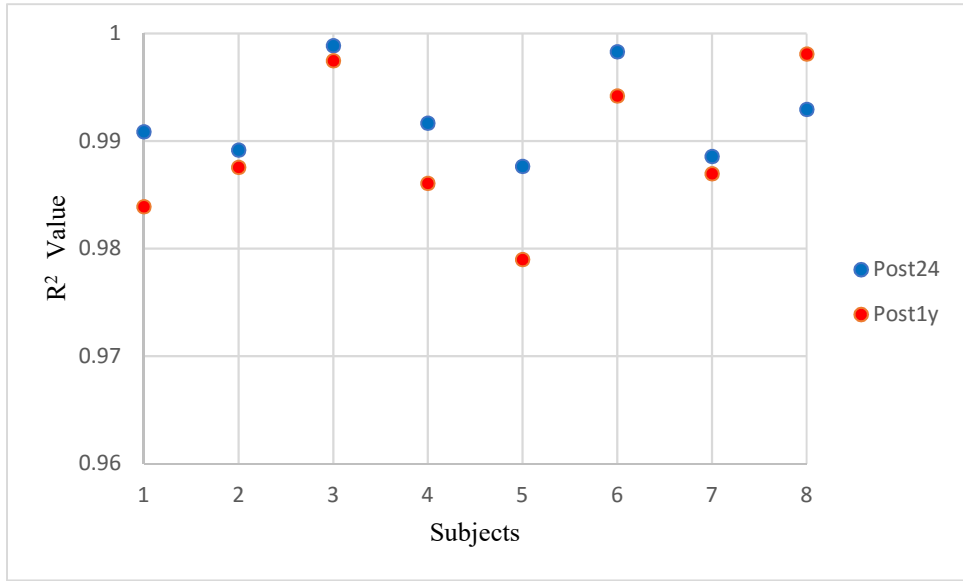
Fig. 3.7: R² values for ROI 5

The outcomes obtained for ROI 3, 4, 5 with the regression analysis are summarized in the following Tables. To compare the results with gain/loss assessment, the percentage of increase (green) or decrease (red) for each parameter is calculated with the formula [3.1]:

$$Diff = \frac{Param\_1y - Param\_24}{Param\_24} \times 100 \qquad [3.1]$$

Patient	SLICE	AMP1	MU1	SIGMA1
#1	Post24	24	1380	104
	Posy1y	20	1332	134
	Diff %	-16.7	-3.5	28.8
#2	Post24	23	1414	92
	Posy1y	22	1411	94
	Diff %	-4.3	-0.2	2.2
#3	Post24	49	1428	77
	Posy1y	41	1435	78
	Diff %	-16.3	0.5	1.3
#4	Post24	33	1534	72
	Posy1y	30	1539	73
	Diff %	-9.1	0.3	1.4
#5	Post24	50	1465	76
	Posy1y	49	1378	80
	Diff %	-2.0	-5.9	5.3
#6	Post24	58	1444	76
	Posy1y	66	1416	69
	Diff %	13.8	-1.9	-9.2
#7	Post24	24	1459	96
	Posy1y	25	1407	78
	Diff %	4.2	-3.6	-18.8
#8	Post24	46	1469	89
	Posy1y	44	1441	91
	Diff %	-4.3	-1.9	2.2

Table 3.4: Parameters for ROI 3

Patient	SLICE	AMP1	MU1	SIGMA1
#1	Post24	27	1447	98
	Posy1y	27	1416	94
	Diff %	0.0	-2.1	-4.1
#2	Post24	31	1505	77
	Posy1y	29	1487	93
	Diff %	-6.5	-1.2	20.8
#3	Post24	51	1453	78
	Posy1y	53	1457	75
	Diff %	3.9	0.3	-3.8
#4	Post24	35	1556	71
	Posy1y	34	1572	74
	Diff %	-2.9	1.0	4.2
#5	Post24	50	1470	84
	Posy1y	43	1426	98
	Diff %	-14.0	-3.0	16.7
#6	Post24	63	1472	77
	Posy1y	68	1457	71
	Diff %	7.9	-1.0	-7.8
#7	Post24	30	1516	77
	Posy1y	17	1434	150
	Diff %	-43.3	-5.4	94.8
#8	Post24	52	1490	78
	Posy1y	48	1458	94
	Diff %	-7.7	-2.1	20.5

Table 3.5: Parameters for ROI 4

Patient	SLICE	AMP1	MU1	SIGMA1
#1	Post24	30	1435	91
	Posy1y	27	1428	89
	Diff %	-10.0	-0.5	-2.2
#2	Post24	22	1504	122
	Posy1y	27	1495	98
	Diff %	22.7	-0.6	-19.7
#3	Post24	48	1459	88
	Posy1y	48	1465	86
	Diff %	0.0	0.4	-2.3
#4	Post24	35	1577	72
	Posy1y	33	1558	72
	Diff %	-5.7	-1.2	0.0
#5	Post24	44	1479	98
	Posy1y	40	1431	98
	Diff %	-9.1	-3.2	0.0
#6	Post24	51	1473	97
	Posy1y	57	1450	84
	Diff %	11.8	-1.6	-13.4
#7	Post24	27	1516	94
	Posy1y	24	1472	89
	Diff %	-11.1	-2.9	-5.3
#8	Post24	53	1493	82
	Posy1y	50	1465	89
	Diff %	-5.7	-1.9	8.5

Table 3.6: Parameters for ROI 5

4. Discussion

Bone quality assessment is an important step in clinical field, especially in patients undergoing THR. In particular, focusing on the BMD variations around the stem can provide useful information about bone architecture and bone remodeling. It is evident the importance of being able to monitor these changes, thus determining where the bone density decreases (loss) and where it increases (gain). For these reasons, clinicians need an affordable tool to evaluate the success of the operation and to examine femur quality during the follow-up period.

In this context, the project born from the synergy between Landspitali – University Hospital of Iceland and the Institute for Biomedical and Neural Engineering of Reykjavík University (RU) aims to develop a standard tool for the clinical assessment of THR patients.

Using CT scans that are taken 24 hours and 1 year post operation, it is possible to create a three-dimensional model of the femur that provides information about volumetric BMD.

Moreover, in this study, a 2D protocol based on standard cross-section and bone profile is designed to examine post-operative bone quality. While the 3D approach requires access to the full femur CT-scans, the analysis derived from single slices can be of particular utility in identifying key changes and overcoming ethical issues linked to extant imaging modalities.

4.1 3D Gain/Loss assessment

The new protocol for 3D assessment is applied to a cohort of 11 patients (8 uncemented, 3 cemented) undergoing THR. For dataset with poor quality image in particular, it is shown how the semi-automatic segmentation can improve the outcomes of the analysis, having a better sensitivity in the areas of BMD changes.

For the first time, this protocol is used to compare femur quality in subjects with different type of fixation, cemented and uncemented, in order to better understand how the two procedures influence the mechanism of bone remodeling, thus providing a strong method to decide which implant allows better clinical performances.

A qualitative analysis of the volumetric distribution can help the clinicians to identify those areas more affected by bone adaptation, isolate zones more susceptible to fracture risk and carry out patient-based strategies to avoid the failure of the prosthesis, such as bisphosphonate treatment to minimize bone loss [56].

Following the work of Pitto et al., 5 ROI are selected in order to perform a 2D assessment. The same CT-scans are used to crop the femur's model in 5 sub-volumes (§2.3.1) in which calculate the percentages of gain and loss. This quantitative evaluation allows to directly compare same volumes of interest in the cohort of patients.

Although the distribution between subjects (age, sex) can be very different, the percentages show encouraging results. In particular, the majority of the patients (both cemented and uncemented) show a considerably reduction of periprosthetic bone in VOI 2 and VOI 3, which is comparable to the results obtained in other studies. [49] [57]

Thanks to the press-fitting of the non-cemented stem achieved by surgery, several studies show that the bone layers at the stem-bone boundaries are preloaded and encouraged to grow and get stronger [58] [28]. The 3D evaluation for the 8 cemented subjects provides similar outcomes, since the highest percentages of gain are registered in VOI 1 and VOI 2. On the contrary, although the number of cemented implant analyzed is low, all 3 patients display a substantial increase of BMD in VOI 5, 2 cm under the tip of the prosthesis.

Limits

Despite the fact that these new steps added to the previous protocol allow a better estimation of gain and loss in the 3D assessment, some limitations on the accuracy remain, due also to the features of the tools used in Mimics.

The semi-automatic segmentation makes the evaluation stronger when the CT-image are of poor quality and provides a 3D model of the femur in which a greater portion of the bone is considered. On the contrary, a method based exclusively on the threshold (255 HU-3070 HU) is not enough to take into account the BMD variability between the patients, in some cases in fact this range of HU leads to discard pixels belonging to the bone. Nevertheless, the mask obtained with the manual segmentation is not standard and can vary each time due to the inter-operator and intra-operator errors.

 The analysis of cemented dataset highlights another limit. Sometimes the pixels with cement have values belonging to the HU threshold, so it is not possible to separate them from real bone and they are considered in the gain/loss assessment. Anyway, if the density changes in the cement after 1 year are negligible, the procedure registration + subtraction can overcome this issue.

The Registration Process is another weakness of the protocol. In Mimics, to overlay the CT-scan, a series of landmarks are selected as reference. Even this step, as explained for the manual segmentation, is affected by a lack of repeatability. Moreover, the only way the software has to assess

gain and loss is to perform the registration + subtraction operation between post 24h and post 1y images twice, thus doubling the above-mentioned problems.
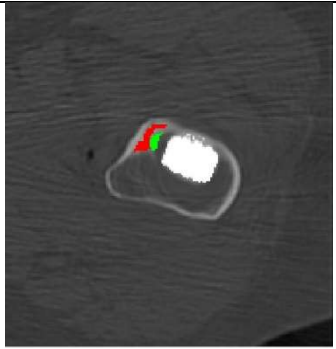
If the registration is poor, a misalignment of the datasets influence the results of the evaluation. As explained in §2.2.4, identifying more landmarks may improve this step, although it leads to amplify intra-operator and inter-operator errors. Another solution proposed in the protocol is to erode the outer layer of the contour mask, considering that an excessive number of eroded pixels produces a loss of information, while a too low number of eroded pixels leads to an overestimation of the BMD changes.
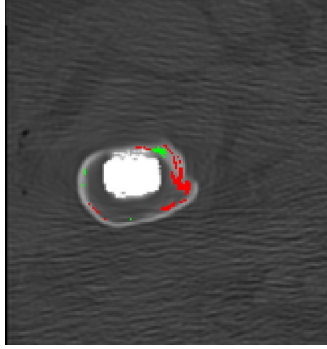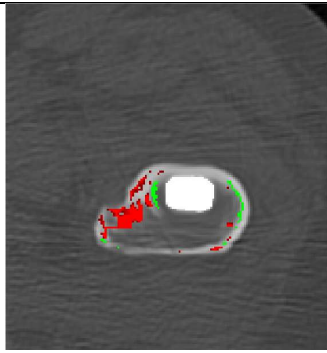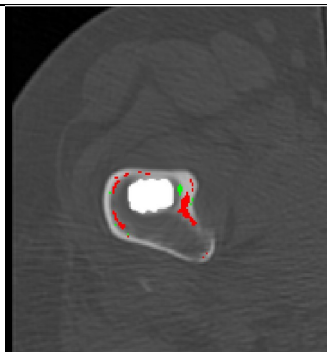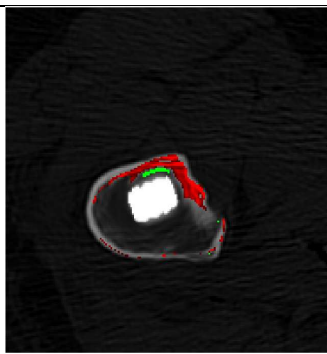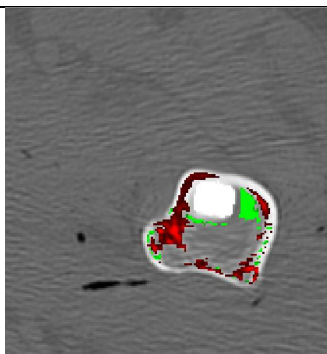
4.2 Cross-section based assessment

4.2.1 Gain/Loss assessment using Matlab Image Processing Toolbox

Using the CT-scans selected for the Bone Profile analysis, a novel procedure is carried out to examine BMD changes in 5 standard ROI. This way, a qualitative and quantitative comparison can be performed examining the areas in which gain and loss are more present. As shown with the 3D assessment, regarding the 8 patients involved, the proximal part of the femur is the most affected by bone remodeling.

Same information can be extracted through the new Matlab approach, considering for example ROI 2 (Tab. 4.1).

PATIENT	Gain/Loss
#1	

#2	
#3	
#4	
#5	
#6	

#7	
#8	
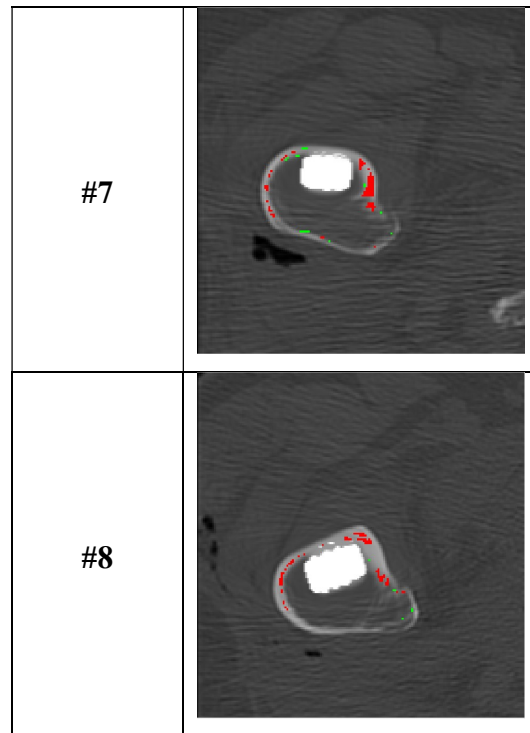
Tab. 4.1: Gain/Loss in ROI2

The results obtained provides the feasibility and the repeatability of the method (having also an automatic and not manually registration), since the same protocol can be applied for different patients, selecting these 5 slices. In particular, the qualitative analysis points out the possibility to get a map of the gain and loss distribution over CT-scans, allowing a visual localization where bone remodeling most occurs. Images show how, in ROI 2, loss is mainly visible in the periprosthetic bone around the lesser trochanter.

Limits

Since this procedure is based on the segmentation performed in Mimics, the same sources of error afflict the assessment in Matlab. Anyway, the main difference between the two approaches regard the Registration Process. The Intensity-Based Algorithm is based on the minimization of the difference in the intensities between corresponding pixels of the two images (Post24 and Posy1y). If the contour mask is significantly different for the same ROI (fig 4.1), the algorithm sometimes does not find the best transformation, cause the images cannot be perfectly superimposed.
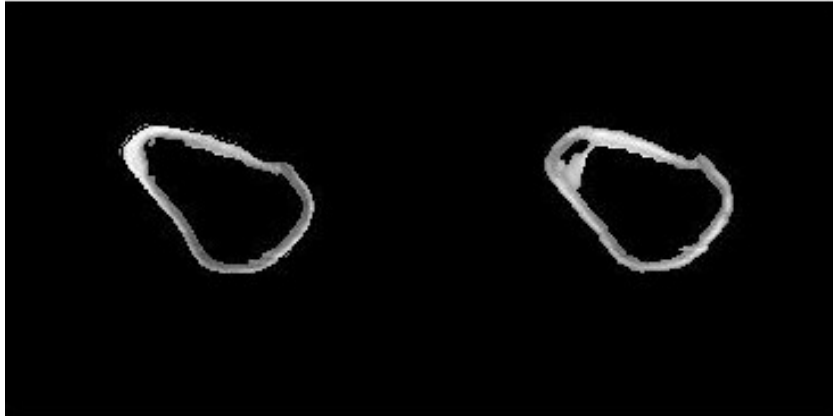
Fig. 4.1: Contour Mask for Greater Trochanter; Post24 (left) and Post1y (right)

As described in the limits paragraph of the 3D assessment, through an erosion of the external layer, it is possible to correct misalignment errors. If qualitatively this solution can be enough to distinguish the areas with BMD changes, the quantitative analysis is clearly more sensible to a failure of the registration. In fact, having few pixels involved in the evaluation (cause only single slices are considered), a little variation on the number of pixels affected by gain or loss implies a great variation on the percentage.

4.2.2 2D Bone Profile

The novelty of this approach is the application to single slices of a standard method based on the analysis of pixels' histogram. Starting from a segmentation performed with specific thresholds on the HU, it is possible to associate a distribution to each type of tissue.
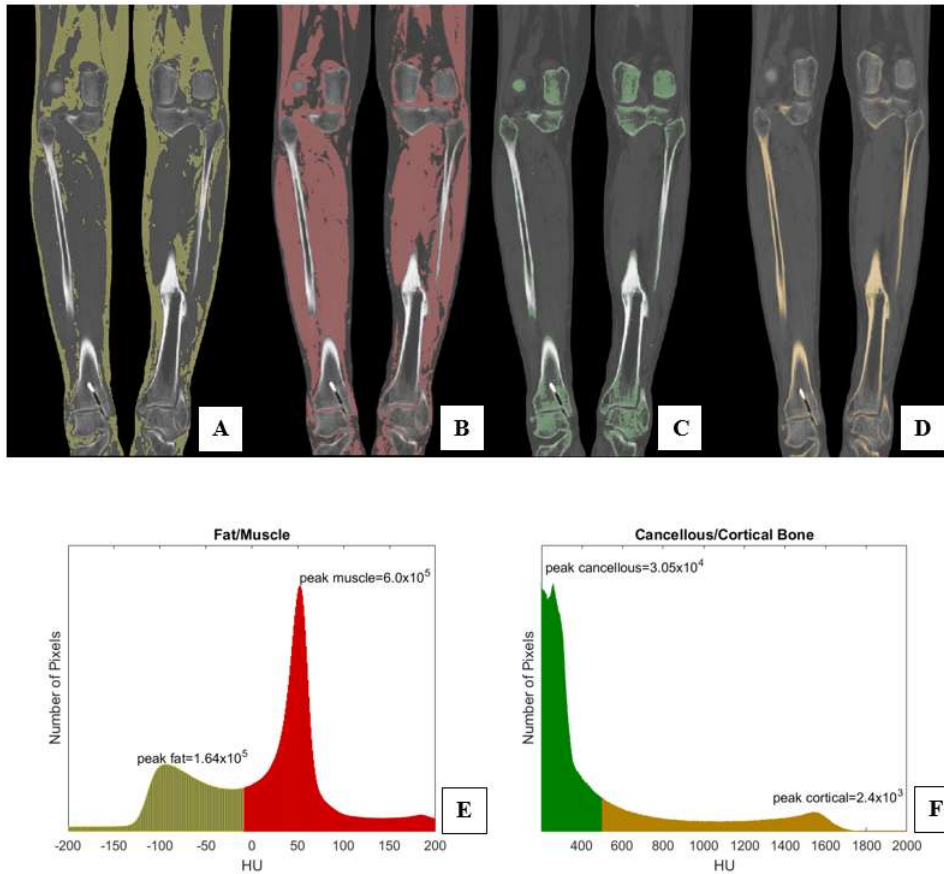
Fig. 4.2: Coronal view from a lower limb section underlining: Fat tissues -200; -10 HU, (A). Water, muscle and connective tissues -9; 200 HU, (B). Bone Cancellous 201; 500 HU, (C). Cortical bone 501; 2000, (D). Hounsfield distributions associated to soft tissues (E) and bone (F).

Recent works have shown the possibility to extract interesting information examining these characteristic profiles [1] [2]. Following similar steps, this work introduces a new procedure to assess bone quality from CT-scans of 5 ROI in patient undergoing THR. Through a process of model fitting, certain parameters can be used to describe the distribution and compare dataset acquired in different times (in this case 24 hours and 1 year after the operation). As shown in §2.3.4, the parameters of the Gaussian regression analysis have a physical meaning that can be correlated to the condition of the bone:

-N (amplitude of the distribution) represents the volume of the tissue;

-μ, σ (location of the distribution's mean and width) are associated to BMD.

58

A modification of these values between Post24 and Post1y profile is clearly linked to a variation of tissue quality. In particular, it is evident that the shift in the mean HU of the Gaussian can be a manifestation of the process of bone remodeling. Actually, from the data available, it is not possible to strongly correlate gain and loss with the assessment of the distribution, however this work demonstrates the feasibility of this new approach.

Limits

There are several limitations concerning the definition of the bone profile. The information extracted from single slices is more easily affected by imperfections in the segmentation. In particular, the Partial Volume Effect (PVE), as described in other works [54] [60], is one of the main source of error, causing a lack of fidelity in the HU values at the interface between two different tissues (as bone and muscle).

Having few pixels for each section, the obtained distribution can be very noisy. A possible solution is the application of a smoothing process, but this operation leads to a loss of information, especially in the peak of the profile (although without such procedure the fitting would not provide a good R^2).

Moreover, the features of the histogram (edges, range of HU) have a great influence in the outcomes of the assessment, so a deeper analysis of these features will be requested in the future.

In conclusion, for the 2D analysis, the limitations are clearly a consequence of the low number of data (image pixels) that can be used in the regression analysis.

5. Future Works and Conclusions

5.1 3D Gain/Loss assessment

The improvement in the 3D assessment shows a better evaluation of BMD changes in comparison with previous protocol. Moreover, it is demonstrated that this approach can be used for the analysis of cemented patients.

Despite the presence of some limits, this procedure may become the standard for the volumetric evaluation of gain and loss. With a greater cohort of subjects, it will be possible to perform statistical analysis and examine the correlation between sex, gender, type of fixation and bone quality. As described in §4.1, the definition of the 5 VOI provides a quantitative description which is comparable with the results of other established methods (such as DEXA).

Future work will also include the application of similar studies to examine BMD in sub-volumes defined in the pre-operative dataset, looking for a correlation between femur quality and fracture risk index in subjects undergoing THR [61], helping the surgery in the implant decision making.

In conclusion, this method represents a valuable tool for clinicians to monitor bone changes around the prosthesis during post-operative follow-up, providing both qualitative and quantitative information whereas other techniques can't allow.

5.2 Cross-section based assessment

Pursuing the aim of developing a procedure both ethically compatible for patients and affordable for clinicians in the evaluation of bone quality, this thesis presents a protocol based on bi-dimensional profiles (density distribution, number of pixels per Hounsfield Unit), obtained from standard CT-scans. Although the analysis, due to the limits described in §4.3.1, show results not strongly correlated to the 3D assessment, it is demonstrated the feasibility of such approach. All the steps introduced in the Materials and Methods chapter can be easily adapted to examine bone quality in subjects with different pathological and non-pathological conditions, not just in the THR field.

The next phase of the research will focus on two targets. The first one is the improvement of the current protocol, in order to solve some of the problems affecting the analysis. Different solutions are already available and need to be tested. The information (in terms of number of pixels) extracted from single slices may not be enough to provide significant results, so the same approach can be used on more CT-scans (e.g. 5 or 10 images), making stronger the model fitting. Another limitation is that each dataset has a different pixel size and consequently a different resolution. It is evident that with a lower pixel size the 2D analysis is improved, possibly leading to more significant outcomes. So, closely linked to this consideration, the main idea is the definition of a scan-protocol that can be adapted to provide a better assessment (standard pixel size, slice thickness...).

On the other side, as explained above, the same approach can be applied to a greater cohort of subjects in different clinical condition to evaluate bone quality.

Along with the 2D assessment, the thesis introduces an alternative protocol based on the registration of single CT-scans, through the Matlab Image Processing Toolbox. Although this evaluation does not provide the same accuracy of the 3D one, it can be valid especially in the region which this study confirms to be more subject to BMD changes (e.g. ROI 2).

After an improvement of the algorithm of registration, the entire procedure (including segmentation) may be exported in Matlab in order to automatize the process.

The ultimate purpose of these cross-section based approaches is the creation of an app that would be a valid and easy-to-use tool in the clinical environment, in order to evaluate bone quality and increase both pre-operative decision making and post-operative rehabilitation strategies.

References

[1] Magnússon, Benedikt, et al. "Improving planning and post-operative assessment for Total Hip Arthroplasty." European journal of translational myology 25.2 (2015).

[2] Coupaud, Sylvie, et al. "Patient-specific bone mineral density distribution in the tibia of individuals with chronic spinal cord injury, derived from multi-slice peripheral Quantitative Computed Tomography (pQCT)—A cross-sectional study." Bone (2016).

[3] Gargiulo, Paolo. "3D Modelling and monitoring of denervated muscle under Functional Electrical Stimulation treatment and associated bone structural change." Eur J Transl Myol-Basic Appl Myol 21 (2011): 31-94.

[4] Gargiulo, Paolo, et al. "Restoration of muscle volume and shape induced by electrical stimulation of denervated degenerated muscles: qualitative and quantitative measurement of changes in rectus femoris using computer tomography and image segmentation." Artificial organs 32.8 (2008): 609-613.

[5] Singh JA. Epidemiology of Knee and Hip Arthroplasty: A Systematic Review. The Open Orthopaedics Journal. 2011 Mar 16;5(1):80–5.

[6] Bottai, Vanna, et al. "Total hip replacement in osteoarthritis: the role of bone metabolism and its complications." Clinical Cases in Mineral and Bone Metabolism 12.3 (2015): 247.

[7] P. Gargiulo and H. Jónsson Jr, «Clinical evaluation score for Total Hip Arthroplasty planning and post-operative assessment» Reykjavik, 2014.

[8] A. Menichetti. "IN SILICO METHODS TO EVALUATE FRACTURE RISK AND BONE MINERAL DENSITY CHANGES IN PATIENTS UNDERGOING TOTAL HIP REPLACEMENT" University of Bologna, 2016.

[9] S. Cowin, W. Buskirk Van, and R. Ashman, ―The properties of bone, in *Handbook of bioengineering*, R. Skalak and S. Chien, Eds. New York: McGraw Hill Companies, 1987.

[10] J. Bilezikian, L. Raisz and T. Martin, Principles of Bone Biology, Academic Press, 2008.

[11] Cristofolini, L. Slides for lessons in "Biological Tissue Mechanics", University of Bologna, 2016.

[12] Raggatt, Liza J., and Nicola C. Partridge. "Cellular and molecular mechanisms of bone remodeling." Journal of Biological Chemistry 285.33 (2010): 25103-25108.

[13] Kini, Usha, and B. N. Nandeesh. "Physiology of bone formation, remodeling, and metabolism." Radionuclide and hybrid bone imaging. Springer Berlin Heidelberg, 2012. 29-57.

[14] Cristofolini, Luca. "In vitro evidence of the structural optimization of the human skeletal bones." Journal of biomechanics 48.5 (2015): 787-796.

[15] Cristofolini, Luca. "A critical analysis of stress shielding evaluation of hip prostheses." Critical Reviews™ in Biomedical Engineering 25.4-5 (1997).

[16] https://www.britannica.com/science/hip [online].

[17] J. R. Lieberman, B. J. Thomas, G. A. M. Finerman, and F. Dorey, "Patients' reasons for undergoing total hip arthroplasty can change over time," The Journal of Arthroplasty, vol. 18, no. 1, pp. 63–68, Jan. 2003.

[18] R. Crawford and D. Murray, «Total hip replacement: indications for surgery and risk factors for failure» Ann Rheum Dis, vol. 56, pp. 455-457, 1997.

[19] R.I.P.O., «HIP, KNEE AND SHOULDER ARTHROPLASTY IN EMILIA ROMAGNA (ITA-LY),» Servizio Sanitario Regionale Emilia-Romagna, 2015.

[20] S. Pramanik, A. Agarwal and K. Rai, "Chronology of Total Hip Joint Replacement and Materials Development," Trends Biomater. Artif. Organs, vol. 19, no. 1, pp. 15-26, 2005.

[21] OECD, «HEALTH AT A GLANCE 2015» 2015.

[22] http://evertsmith.com/innovations/.

[23] Zimmer, "CLS Spotorno Hip Stem Surgical Technique," Zimmer.

[24] http://www.healthpages.org/surgical-care/hip-joint-replacement-surgery/.

[25] http://www.healthpages.org/surgical-care/hip-joint-replacement-surgery/.

[26] Bishop, N. E., S. Ferguson, and S. Tepic. "Porosity reduction in bone cement at the cement-stem interface." Bone & Joint Journal 78.3 (1996): 349-356.

[27] Herberts, Peter, and Henrik Malchau. "Long-term registration has improved the quality of hip replacement: a review of the Swedish THR Register comparing 160,000 cases." Acta Orthopaedica Scandinavica 71.2 (2000): 111-121.

[28] Yamada, Harumoto, et al. "Cementless total hip replacement: past, present, and future." Journal of Orthopaedic science 14.2 (2009): 228-241.

[29] Engh, Charles A., et al. "Results of cementless revision for failed cemented total hip arthroplasty." Clinical orthopaedics and related research 235 (1988): 91-110.

[30] Engelbrecht, D. J., et al. "Long-term results of revision total hip arthroplasty." Bone & Joint Journal 72.1 (1990): 41-45.

[31] A. Abdulkarim, P. Ellanti and al., "Cemented versus uncemented fixation in total hip replacement: a systematic review and meta-analysis of randomized controlled trials" *Orthop Rev,* no. 5, 2013.

[32] Adams, Judith E. "Quantitative computed tomography." European journal of radiology 71.3 (2009): 415-424.

[33] R. Ciernak, X-ray Computed Tomography in Biomedical Engineering, London: Springer-Verlag, 2011.

[34] L. Goldman, «Principles of CT and CT Technology» Journal of Nuclear Medicine Technology, vol. 35, pp. 115-128, 2007.

[35] Cristofolini, L., et al. "Preclinical assessment of the long-term endurance of cemented hip stems. Part 1: Effect of daily activities-a comparison of two load histories." Proceedings of the Institution of Mechanical Engineers, Part H: Journal of Engineering in Medicine 221.6 (2007): 569-584.

[36] Cristofolini, L., et al. "Preclinical assessment of the long-term endurance of cemented hip stems. Part 2: in-vitro and ex-vivo fatigue damage of the cement mantle." Proceedings of the Institution of Mechanical Engineers, Part H: Journal of Engineering in Medicine 221.6 (2007): 585-599.

[37] E. Mirsky and T. Einhorn, «Bone densitometry in orthopaedic practice» J Bone Joint Surg Am, vol. 80, n. 11, pp. 1687-1698, 1998.

[38] R. Schmidt, L. Muller, A. Kress, H. Hirschfelder, A. Aplas and R. Pitto, «A computed tomography assessment of femoral and acetabular bone changes after total hip arthroplasty» Int Orthop, vol. 26, n. 5, pp. 299-302, 2002.

[39] Gargiulo, Paolo, et al. "Assessment of total hip arthroplasty by means of computed tomography 3D models and fracture risk evaluation." Artificial organs 37.6 (2013): 567-573.

[40] Pétursson Þ, Edmunds KJ, Gíslason MK, Magnússon B, Magnúsdóttir G, Halldórsson G, Jónsson H Jr, Gargiulo P. "Bone Mineral Density and Fracture Risk Assessment to Optimize Prosthesis Selection in Total Hip Replacement". Comput Math Methods Med. 2015

[41] Pétursson, Þröstur, et al. "Bone and muscle assessment in patients undergoing total hip arthroplasty using HU based analysis." European Journal of Translational Myology 22.3 (2012): 147-152.

[42] Gargiulo, Paolo, et al. "Bone Mineral Density and Fracture risk assessment for patients undergoing total hip arthroplasty as support for decision making." European International Journal of Science and Technology 2.5 (2013): 96-105.

[43] Edmunds, Kyle Joseph, et al. "Multimodal Quantitative Assessment for Pre-operative Prosthesis Selection in Total Hip Arthroplasty." XIV Mediterranean Conference on Medical and Biological Engineering and Computing 2016. Springer International Publishing, 2016.

[44] R. Schmidt, L. Muller, A. Kress, H. Hirschfelder, A. Aplas and R. Pitto, «A computed tomography assessment of femoral and acetabular bone changes after total hip arthroplasty» *Int Orthop,* vol. 26, n. 5, pp. 299-302, 2002.

[45] Þ. Hermannsson and P. Gargiulo, "Phantom protocol for segmentation and bone apparent density calculation," University of Reykjavik, 2016.

[46] R. Radiology, «Metal Deletion Technique (MDT) - ReVision Radiology».

[47] Boas, F. Edward, and Dominik Fleischmann. "Evaluation of two iterative techniques for reducing metal artifacts in computed tomography." Radiology 259.3 (2011): 894-902.

[48] Benedikt Magnússon, "Development of Clinical Assessment strategies for patients undergoing Total Hip Arthroplasty (THA)", Reykjavik University Master Thesis, 2013.

[49] R. P. Pitto et al., «Femoral bone density changes after total hip arthroplasty with uncemented taper-design stem: a five-year follow-up study» International Orthopaedics, n. 34, pp. 783-787, 2010.

[50] MR. D.P. KHUNT, PROF. Y.N.MAKWANA, "Image Registration Using Intensity Based Technique".

[51] https://se.mathworks.com/help/images/intensity-based-automatic-image-registration.html

[52] Joseph V. Hajnal, Derek L.G. Hill, "Medical image registration" CRC Press, Jun 27, 2001

[53] Edmunds, Kyle Joseph, et al. "Quantitative Computed Tomography and image analysis for advanced muscle assessment." European Journal of Translational Myology 26.2 (2016).

[54] Edmunds, K. J., et al., "Nonlinear Trimodal Regression Analysis of Radiodensitometric Distributions to Quantify Sarcopenic and Sequelae Muscle Degeneration." Computational and Mathematical Methods in Medicine 2016 (2016).

[55] Menichetti, A., Gargiulo, P., Gislason, M., Edmunds, K., Hermannsson, T., Jonsson, H., Esposito, L., Bifulco, P., Cesarelli, M., Fraldi, M., & Cristofolini, L. (2017). ASSESSMENT METHOD FOR FRACTURE RISK AND BONE MINERAL DENSITY CHANGES AS

SUPPORT FOR IMPLANT DECISION MAKING IN TOTAL HIP REPLACEMENT. Bone Joint J, 99-B(SUPP 2), 111.

[56] Prieto-Alhambra, Daniel, et al. "Fracture risk before and after total hip replacement in patients with osteoarthritis: potential benefits of bisphosphonate use." Arthritis & Rheumatism 63.4 (2011): 992-1001.

[57] Dan, Diana, et al. "Bone loss after total hip arthroplasty." Rheumatology international 26.9 (2006): 792-798.

[58] J. McLaughlin, «Total Hip Arthroplasty with an Uncemented Tapered Femoral Component» The Journal of Bone and Joint Surgery (American), vol. 90, n. 6, pp. 1290-1296, 2008.

[59] Lévy, S., Benhamou, M., Naaman, C., Rainville, P., Callot, V., & Cohen-Adad, J. (2015). White matter atlas of the human spinal cord with estimation of partial volume effect. NeuroImage, 119, 262–271.

[60] Þröstur Hermannsson, "Bone Model to Optimize Implant Selection in Total Hip Arthroplasty", Reykjavik University Master Thesis, 2017

Appendix A

Matlab Code for Image Registration

```
close all
clear all
clc

% automatic intensity-based registration
%Load one of the slices (GT-Grater trochanter)
Post24=load('GT_post24  .mat');
Post1y=load('GT_post1y  .mat');

[m n]=size(Post24.original);

%saving original images
Post24_original=Post24.original;
Post1y_original=Post1y.original;

%load contour mask (it can be imported on the dicom file from Mimics) to implement better
registration
Post24cn=load('GTcn_post24  .mat');
Post1ycn=load('GTcn_post1y  .mat');

%apply the mask to the image
Post24=Post24.original.*Post24cn.contour;
Post1y=Post1y.original.*Post1ycn.contour;


figure
imshowpair(Post24,Post1y,'montage')

%erosion for error of the registration
%true(3) 1 eroded
%true(5) 2 eroded
%true(7) 3 eroded
cn24_er=imerode(Post24cn.contour, true(5));
cn1y_er=imerode(Post1ycn.contour, true(5));

figure
imshowpair(Post24_original,Post1y_original,'montage')
title('Unregistered Post24/Post1y')
```

```matlab
%registration options
[optimizer,metric] = imregconfig('monomodal');


%using imregtform to have the transform in output
[R_REG] = imregtform(Post1y, Post24, 'affine', optimizer, metric);

%apply the registration
Post1y_or_reg = imwarp(Post1y_original,R_REG,'OutputView',imref2d(size(Post24)));
Post1y_reg = imwarp(Post1y, R_REG,'OutputView',imref2d(size(Post24)));
figure
imshowpair(Post1y_or_reg, Post24_original)
title ('A: Intensity-based registration Post1y on Post24')

%loss assessment
delta_loss=Post24-Post1y_or_reg;

%load contour_eroded mask
delta_loss=delta_loss.*cn24_er;

%gain assessment
delta_gain=Post1y_or_reg-Post24_original;


%register contour eroded mask post1y

mask_gain=imwarp(cn1y_er,R_REG,'OutputView',imref2d(size(Post24)));
delta_gain=delta_gain.*mask_gain;

%mask for figure representation
red_mask=zeros(m,n);
green_mask=zeros(m,n);

%threshold on deltaGV_significant
for i=1:m
  for j=1:n
    red_mask(i,j)=1;
    green_mask(i,j)=1;
    if delta_gain(i,j)<111
      delta_gain(i,j)=0;
      green_mask(i,j)=0;

    end
    if delta_loss(i,j)<111
      delta_loss(i,j)=0;
      red_mask(i,j)=0;
    end
```

```matlab
    end
end

%loss percentage
pixel_loss=nnz(delta_loss);
pixel_post24=nnz(Post24);
loss=pixel_loss/pixel_post24*100;

%gain percentage
pixel_gain=nnz(delta_gain);
pixel_post1y=nnz(Post1y);
gain=pixel_gain/pixel_post1y*100;

%unknown loss/gain
unknown=100-loss-gain;
```

Acknowledgments

First of all, I would like to thank my supervisor Prof. Luca Cristofolini for giving me the opportunity to take part in a study experience in Iceland and for his helpful suggestions during my time writing this thesis.

I would like to express my gratitude to Prof. Paolo Gargiulo for hosting me at Reykjavik University. It has been a great experience working with him. His help was fundamental for the whole project.

I would like to thank Magnús Kjartan Gíslason, assistant professor at University of Reykjavik. He was always ready to assist and has been a good support of this work.

I would like to thank all the people I collaborated with during the stay at Reykjavik University.

Thanks to my colleagues and all my friends, especially Giulio and Filippo, because they encouraged me during the difficult periods.

Last but not least, I would like to thank my family for their on-going support with words and deeds during my whole university career.